NNLL fit of the unpolarised gluon TMD PDF

to LHCb data on J/ψ-pair production

Based on arXiv:**2609.01000**

D. Boer, J. Bor, A.Colpani Serri, M.G. Echevarria, J.P. Lansberg, **SFR**, P. Taels



Resummation, Evolution and Factorization

Samuel F. Romera

IGFAE, Santiago de Compostela (Spain)

19-23 Oct 2026

EHU | Qc EHU Quantum Center

TMD extractions

TMD extractions

- TMD factorisation at $q_T \ll Q$ is established for **Drell–Yan** and **SIDIS** → quark TMDs from global fits.

TMD extractions

- TMD factorisation at $q_T \ll Q$ is established for **Drell–Yan** and **SIDIS** → quark TMDs from global fits
- Two decades of progress: Gaussian/NLL fits → **N³LL–N⁴LL** analyses of ∼10^3 points; flavour dependence, neural networks, CS kernel vs lattice

Semi-inclusive DIS $\ell N \to \ell' h X$ — 8 experiments

TMD PDF × TMD FF — 3 completed · 1 running · 4 future

●	**HERMES** DESY	1995–2007	◌	**SoLID** JLab	*planned*
●	**COMPASS** CERN	2002–2022	◌	**JLab 22 GeV** JLab	*proposed*
●	**CLAS** JLab	1998–2012	◌	**ePIC** BNL	*2030s*
◉	**CLAS12, Halls A/C** JLab	2018–	◌	**EicC** IMP-CAS	*proposed*

Drell–Yan $h_1 h_2 \to \ell^+ \ell^- X$ — 9 experiments

TMD PDF × TMD PDF — 3 completed · 5 running · 1 future

●	**COMPASS** CERN	2015, 2018	◉	**ATLAS** CERN	2010–
●	**SeaQuest** Fermilab	2014–2017	◉	**CMS** CERN	2010–
●	**STAR** BNL	2000–2026	◉	**LHCb** CERN	2010–
◉	**AMBER** CERN	2023–2031	◌	**LHCspin** CERN	*proposed*
◉	**SpinQuest** Fermilab	2024–			

e^+e^- annihilation $e^+e^- \to h_1 h_2 X$ — 4 experiments

TMD FF × TMD FF — 2 completed · 2 running

●	**BaBar** SLAC	1999–2008	◉	**Belle II** KEK	2019–
●	**Belle** KEK	1999–2010	◉	**BESIII** IHEP	2009–

pp, *pA* collisions — 7 experiments

Gluon TMDs — 3 completed · 3 running · 1 future

●	**PHENIX** BNL	2000–2016	◉	**CMS** CERN	2010–
●	**STAR** BNL	2000–2026	◉	**LHCb** ★ CERN	2010–
●	**sPHENIX** BNL	2023–2026	◌	**SPD** JINR	*planned*
◉	**ATLAS** CERN	2010–			

● completed ◉ running ◌ planned or proposed ★ J/ψ-pair data used in this talk

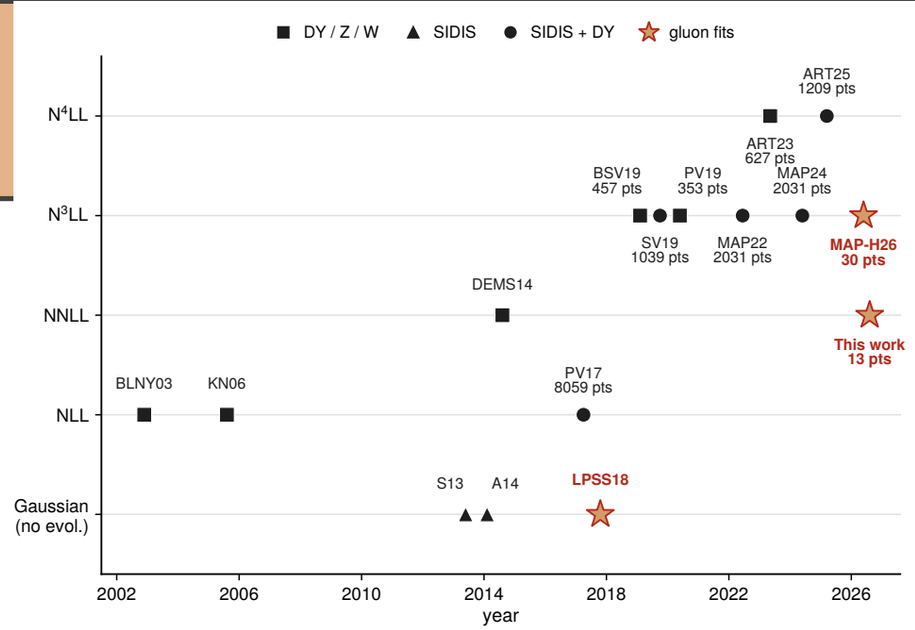
Status as of October 2026

Quark TMD fits: BLNY03 Landry et al., PRD 67 (2003) 073016 · KN06 Konychev, Nadolsky, PLB 633 (2006) 710 · S13 Signori et al., JHEP 11 (2013) 194 · A14 Anselmino et al., JHEP 04 (2014) 005 · DEMS14 D'Alesio et al., JHEP 11 (2014) 098 · PV17 Bacchetta et al., JHEP 06 (2017) 081 · BSV19 Bertone, Scimemi, Vladimirov, JHEP 06 (2019) 028 · SV19 Scimemi, Vladimirov, JHEP 06 (2020) 137 · PV19 Bacchetta et al., JHEP 07 (2020) 117 · MAP22 JHEP 10 (2022) 127 · ART23 Moos et al., JHEP 05 (2024) 036 · MAP24 JHEP 08 (2024) 232 · MAPNN PRL 135 (2025) 021904 · ART25 Moos et al., JHEP 11 (2025) 134

Gluon TMD fits: LPSS18 Lansberg, Pisano, Scarpa, Schlegel, PLB 784 (2018) 217 · MAP-H26 Anedda, Bertone, Bozzi, Cerutti, arXiv:2605.28216 · This work: Boer et al., arXiv:2609.01000

TMD extractions

- TMD factorisation at $q_T \ll Q$ is established for **Drell–Yan** and **SIDIS** → quark TMDs from global fits
- Two decades of progress: Gaussian/NLL fits → **N³LL–N⁴LL** analyses of ~10^3 points; flavour dependence, neural networks, CS kernel vs lattice



Semi-inclusive DIS $\ell N \to \ell' h X$ — 8 experiments

TMD PDF × TMD FF — 3 completed · 1 running · 4 future

●	**HERMES** DESY	1995–2007	◌	**SoLID** JLab	*planned*
●	**COMPASS** CERN	2002–2022	◌	**JLab 22 GeV** JLab	*proposed*
●	**CLAS** JLab	1998–2012	◌	**ePIC** BNL	*2030s*
◉	**CLAS12, Halls A/C** JLab	2018–	◌	**EicC** IMP-CAS	*proposed*

Drell–Yan $h_1 h_2 \to \ell^+ \ell^- X$ — 9 experiments

TMD PDF × TMD PDF — 3 completed · 5 running · 1 future

●	**COMPASS** CERN	2015, 2018	◉	**ATLAS** CERN	2010–
●	**SeaQuest** Fermilab	2014–2017	◉	**CMS** CERN	2010–
●	**STAR** BNL	2000–2026	◉	**LHCb** CERN	2010–
◉	**AMBER** CERN	2023–2031	◌	**LHCspin** CERN	*proposed*
◉	**SpinQuest** Fermilab	2024–			

e^+e^- annihilation $e^+e^- \to h_1 h_2 X$ — 4 experiments

TMD FF × TMD FF — 2 completed · 2 running

●	**BaBar** SLAC	1999–2008	◉	**Belle II** KEK	2019–
●	**Belle** KEK	1999–2010	◉	**BESIII** IHEP	2009–

pp, *pA* collisions — 7 experiments

Gluon TMDs — 3 completed · 3 running · 1 future

●	**PHENIX** BNL	2000–2016	◉	**CMS** CERN	2010–
●	**STAR** BNL	2000–2026	◉	**LHCb** ★ CERN	2010–
●	**sPHENIX** BNL	2023–2026	◌	**SPD** JINR	*planned*
◉	**ATLAS** CERN	2010–			

● completed ◉ running ◌ planned or proposed ★ J/ψ-pair data used in this talk

Status as of October 2026

Quark TMD fits: BLNY03 Landry et al., PRD 67 (2003) 073016 · KN06 Konychev, Nadolsky, PLB 633 (2006) 710 · S13 Signori et al., JHEP 11 (2013) 194 · A14 Anselmino et al., JHEP 04 (2014) 005 · DEMS14 D'Alesio et al., JHEP 11 (2014) 098 · PV17 Bacchetta et al., JHEP 06 (2017) 081 · BSV19 Bertone, Scimemi, Vladimirov, JHEP 06 (2019) 028 · SV19 Scimemi, Vladimirov, JHEP 06 (2020) 137 · PV19 Bacchetta et al., JHEP 07 (2020) 117 · MAP22 JHEP 10 (2022) 127 · ART23 Moos et al., JHEP 05 (2024) 036 · MAP24 JHEP 08 (2024) 232 · MAPNN PRL 135 (2025) 021904 · ART25 Moos et al., JHEP 11 (2025) 134

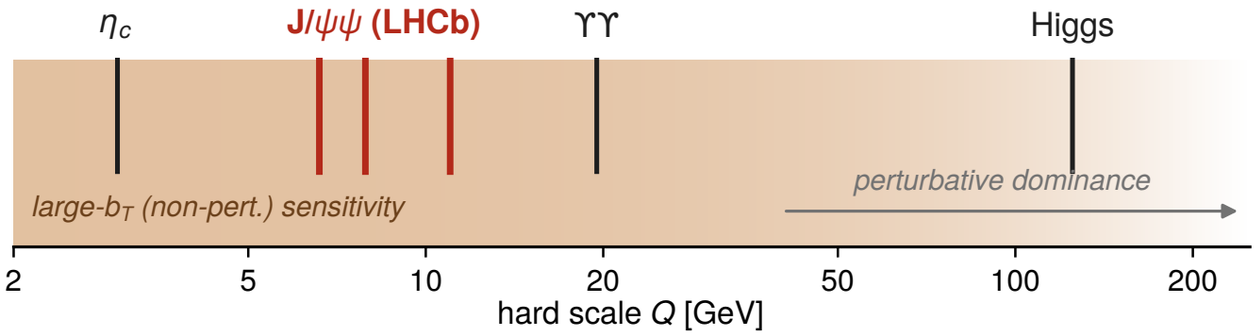
Gluon TMD fits: LPSS18 Lansberg, Pisano, Scarpa, Schlegel, PLB 784 (2018) 217 · MAP-H26 Anedda, Bertone, Bozzi, Cerutti, arXiv:2605.28216 · This work: Boer et al., arXiv:2609.01000

Next frontier: extraction of the gluon TMDs

Quarkonia as tools

Quarkonia as tools

- Gluon TMDs need **gluon fusion** into a **colour-singlet** final state at $q_T \ll Q$
- **Higgs**: clean, but $Q = M_H \rightarrow$ mostly perturbative, weak sensitivity to the non-perturbative gluon structure
- **Quarkonia**: Probe the large-b_T region; large LHC yields, clean $\mu^+\mu^-$ signal.

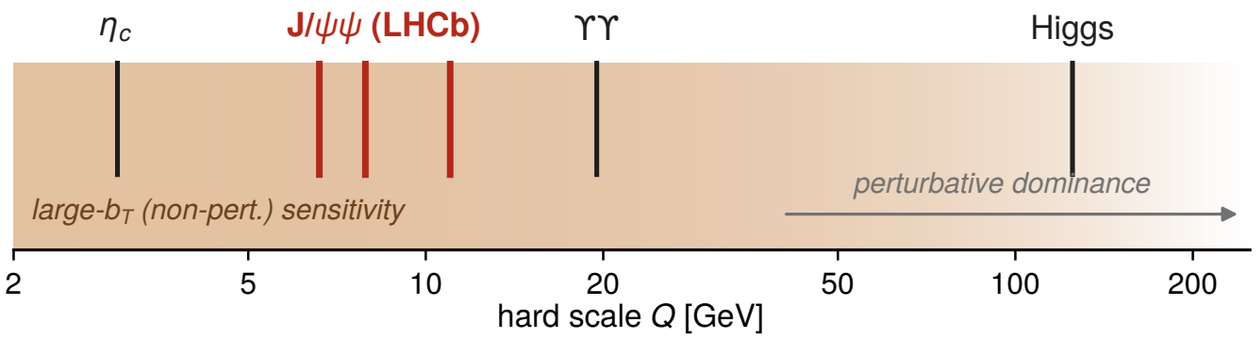


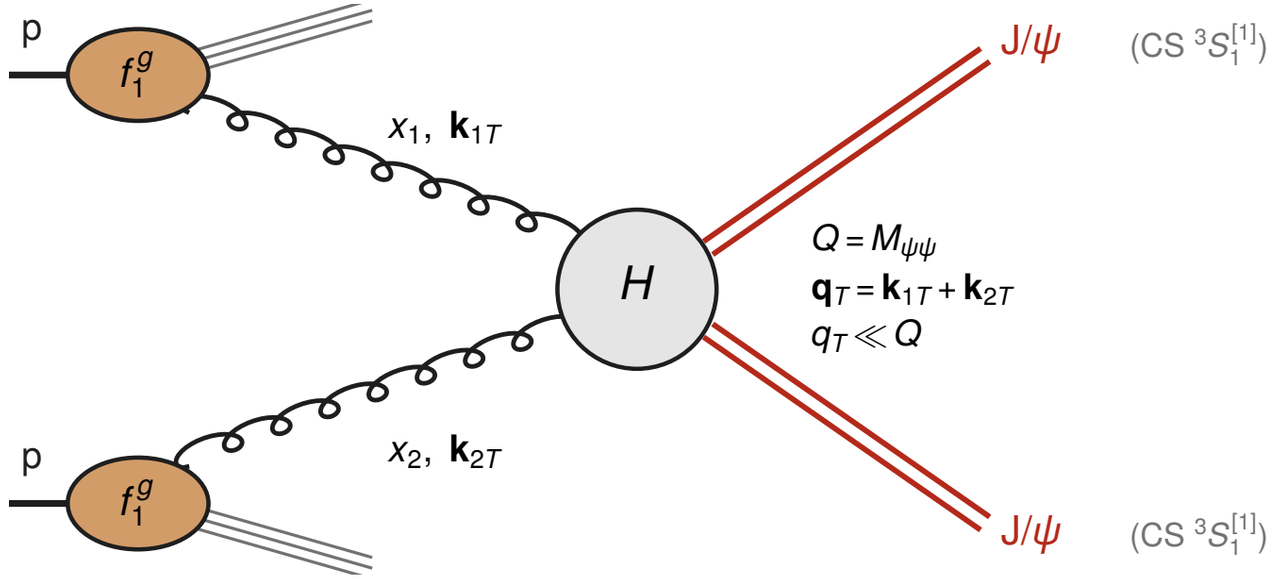
Gluon TMDs: Mulders, Rodrigues, PRD 63 (2001) 094021 · Echevarria, Kasemets, Mulders, Pisano, JHEP 07 (2015) 158 · **Quarkonium in TMD factorisation:** Echevarria, JHEP 10 (2019) 144 · Fleming, Makris, Mehen, JHEP 04 (2020) 122 · Echevarria, Makris, Scimemi, JHEP 10 (2020) 164

J/ψ pairs: Lansberg, Pisano, Scarpa, Schlegel, PLB 784 (2018) 217 (LO Gaussian fit: $\langle k_T^2 \rangle = 3.3 \pm 0.8$ GeV^2) · Scarpa et al., EPJC 80 (2020) 87 · Colpani Serri et al., arXiv:2403.00640 · **Data:** LHCb, JHEP 06 (2017) 047 · LHCb, JHEP 03 (2024) 088 · **Higgs:** MAP, arXiv:2605.28216

Quarkonia as tools

- Gluon TMDs need **gluon fusion** into a **colour-singlet** final state at $q_T \ll Q$
- **Higgs**: clean, but $Q = M_H \rightarrow$ mostly perturbative, weak sensitivity to the non-perturbative gluon structure
- **Quarkonia**: Probe the large-b_T region; large LHC yields, clean $\mu^+\mu^-$ signal
- **J/ψ pairs**: $gg \rightarrow J/\psi\, J/\psi$
- Several bins in $Q = M_{\psi\psi} \rightarrow$ handle on **TMD evolution**: NP gluon Collins–Soper kernel directly from data





Gluon TMDs: Mulders, Rodrigues, PRD 63 (2001) 094021 · Echevarria, Kasemets, Mulders, Pisano, JHEP 07 (2015) 158 · **Quarkonium in TMD factorisation:** Echevarria, JHEP 10 (2019) 144 · Fleming, Makris, Mehen, JHEP 04 (2020) 122 · Echevarria, Makris, Scimemi, JHEP 10 (2020) 164

J/ψ pairs: Lansberg, Pisano, Scarpa, Schlegel, PLB 784 (2018) 217 (LO Gaussian fit: $\langle k_T^2 \rangle = 3.3 \pm 0.8$ GeV^2) · Scarpa et al., EPJC 80 (2020) 87 · Colpani Serri et al., arXiv:2403.00640 · **Data:** LHCb, JHEP 06 (2017) 047 · LHCb, JHEP 03 (2024) 088 · **Higgs:** MAP, arXiv:2605.28216

Goal: NNLL fit of f_1^g to LHCb J/ψ-pair data

Methodology

Data: LHCb prompt J/ψ-pair production

13 TeV
pp collisions · JHEP 03 (2024) 088

3
Q bins: $\langle M_{\psi\psi} \rangle$ = 6.6, 7.9, 11 GeV

13
points with $q_T/\langle M_{\psi\psi} \rangle < 0.5$

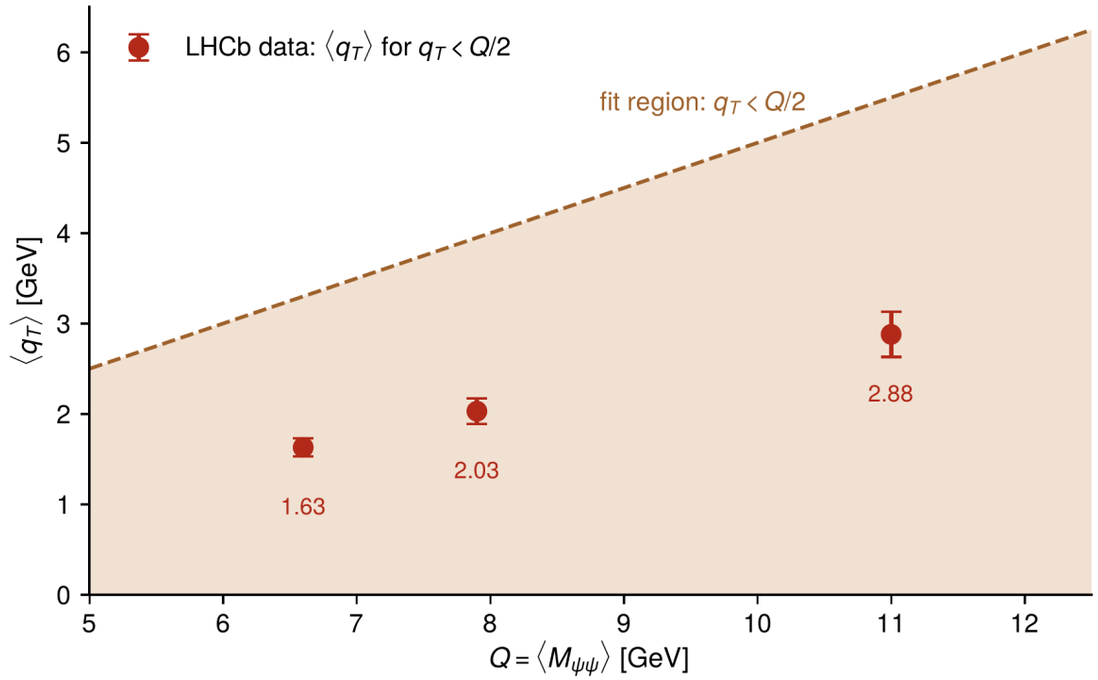
2 – 4.5
pair rapidity $y_{\psi\psi}$

From the measurement to the fit input

1. **Measured double-differentially**
   in $Q = M_{\psi\psi}$ and $q_T = P_{T,\psi\psi}$
2. **DPS subtracted by LHCb**
   via its broader Δy distribution (normalised at $1.8 < \Delta y < 2.5$)
3. **TMD region only**
   $q_T/\langle M_{\psi\psi} \rangle < 0.5 \rightarrow$ 13 data points
4. **Self-normalised in each Q bin**
   hard factor, LDMEs and normalisation uncertainties cancel
5. **Full uncertainty treatment**
   stat. uncorrelated, syst. correlated → one covariance matrix per Q bin
6. **Integrated over φ_{CS}**
   $h_1^{\perp g}$ contributes < 0.5% → sensitive to f_1^g only

Fitted observable: self-normalised q_T spectrum

$$\frac{1}{\sigma}\frac{\mathrm{d}\sigma}{\mathrm{d}q_T} \equiv \left(\int_0^{Q/2} \mathrm{d}q_T \, \frac{\mathrm{d}\sigma}{\mathrm{d}q_T} \right)^{-1} \frac{\mathrm{d}\sigma}{\mathrm{d}q_T}$$



$\langle q_T \rangle$ grows with Q: broadening from TMD evolution, visible directly in the data.

13 points at three values of Q: sensitivity to NP effects and to TMD evolution

CSS formalism

Factorisation

$$\frac{d\sigma}{dQdyd^2q_Td\Omega} \propto \mathscr{C}[f_1^g f_1^g](x_{1,2}, q_T; \mu)$$

see Pieter's talk

Hankel transform

$$\mathcal{C}[f_1^g f_1^g](x_{1,2}, q_T) = \int_0^\infty \frac{\mathrm{d}b_T}{2\pi}\, b_T\, J_0(b_T q_T)\; \tilde{f}_1^g(x_1, b_T; \zeta_1, \mu)\, \tilde{f}_1^g(x_2, b_T; \zeta_2, \mu)$$

Multiplicative evolution

$$\tilde{f}_1^g(x, b_T; Q^2, Q) = \tilde{f}_1^g(x, b_T; \mu_b^2, \mu_b)\; e^{-\frac{1}{2}S_{\mathrm{P}}(b_T; Q^2, Q, \mu_b^2, \mu_b)}, \qquad \mu_b = \frac{b_0}{b_T}$$

Matching at small b_T

$$\tilde{f}_1^g(x, b_T; \mu_b^2, \mu_b) = \sum_{j=q,\bar{q},g} C_{g/j}(x, b_T; \mu_b) \otimes f_1^j(x; \mu_b) \;+\; \mathcal{O}(b_T \Lambda_{\mathrm{QCD}})$$

CSS formalism

Factorisation

$$\frac{d\sigma}{dQdyd^2q_Td\Omega} \propto \mathscr{C}[f_1^g f_1^g](x_{1,2}, q_T; \mu)$$

see Pieter's talk

Hankel transform

$$\mathcal{C}[f_1^g f_1^g](x_{1,2}, q_T) = \int_0^\infty \frac{\mathrm{d}b_T}{2\pi}\, b_T\, J_0(b_T q_T)\; \tilde{f}_1^g(x_1, b_T; \zeta_1, \mu)\, \tilde{f}_1^g(x_2, b_T; \zeta_2, \mu)$$

Multiplicative evolution

$$\tilde{f}_1^g(x, b_T; Q^2, Q) = \tilde{f}_1^g(x, b_T; \mu_b^2, \mu_b)\; e^{-\frac{1}{2}S_{\mathrm{P}}(b_T; Q^2, Q, \mu_b^2, \mu_b)}, \qquad \mu_b = \frac{b_0}{b_T}$$

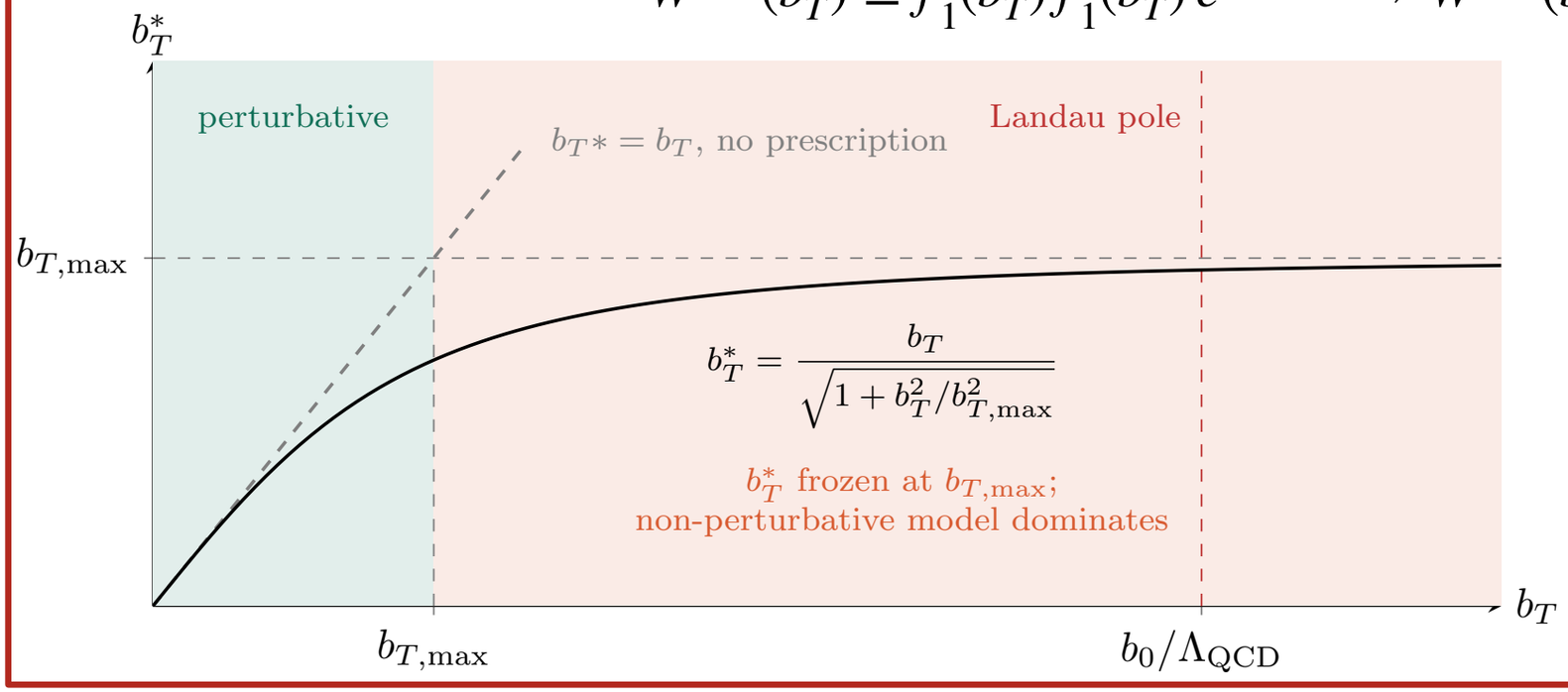
Matching at small b_T

$$\tilde{f}_1^g(x, b_T; \mu_b^2, \mu_b) = \sum_{j=q,\bar{q},g} C_{g/j}(x, b_T; \mu_b) \otimes f_1^j(x; \mu_b) \;+\; \mathcal{O}(b_T \Lambda_{\mathrm{QCD}})$$

⚠ **But $\int db_T$ runs to ∞, while $\mu_b \to \Lambda_{\mathrm{QCD}}$ at large b_T ⇒ a prescription and an NP model are unavoidable**

Non-perturbative input: three choices, all of them matter

$$W^{\mathrm{pert}}(b_T) \equiv \tilde{f}_1^g(b_T)\tilde{f}_1^g(b_T)\, e^{-S_{\mathrm{P}}(b_T)} \to W^{\mathrm{pert}}(b_T^*)\, e^{-S_{\mathrm{NP}}(b_T)}$$



What to add: S_{NP}

$$S_{\mathrm{NP}} = \left(A \ln \frac{Q}{Q_{\mathrm{NP}}} + B\right) b_T^2$$

A ↔ NP Collins–Soper kernel, B ↔ intrinsic part. S_{NP} must **compensate** the b_T^* shift, not rewrite W^{pert}

Distorting the perturbative part

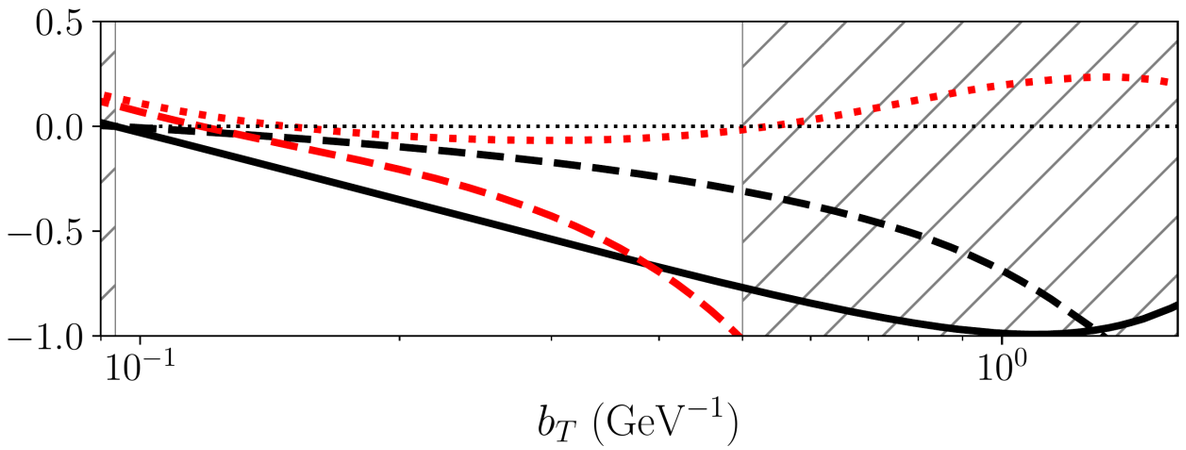
Distorting the perturbative part

Test: $S_P(b_T^*) + S_{NP}(b_T) \simeq S_P(b_T)$ in the perturbative region: $[b_0/Q, b_{T,max}]$ · $b_{T,max} = 0.5\ \text{GeV}^{-1}$, S_{NP} from a quark fit × C_A/C_F or × ½

Reminder: $$W^{\text{pert}}(b_T) \equiv \tilde{f}_1^g(b_T)\,\tilde{f}_1^g(b_T)\,e^{-S_{\text{P}}(b_T)} \to W^{\text{pert}}(b_T^*)\,e^{-S_{\text{NP}}(b_T)} = \tilde{f}_1^g(b_T^*)\,\tilde{f}_1^g(b_T^*)\,e^{-S_{\text{p}}(b_T^*)-S_{\text{NP}}(b_T)}$$

Sudakov exponent: NP shift vs perturbative shifts

Q = 12 GeV (J/ψ pairs), $b_{T,max} = 0.5\ \text{GeV}^{-1}$; white = perturbative region



✗ **Casimir-scaled S_{NP}** (red dashed) deviates far more than LL → NLL → NNLL (black); only the ½-scaled one (dotted) roughly complies → outcome hinges on an S_{NP} not known a priori

Not a truncation effect: conventional b_T^* + S_{NP} rewrites the perturbative input

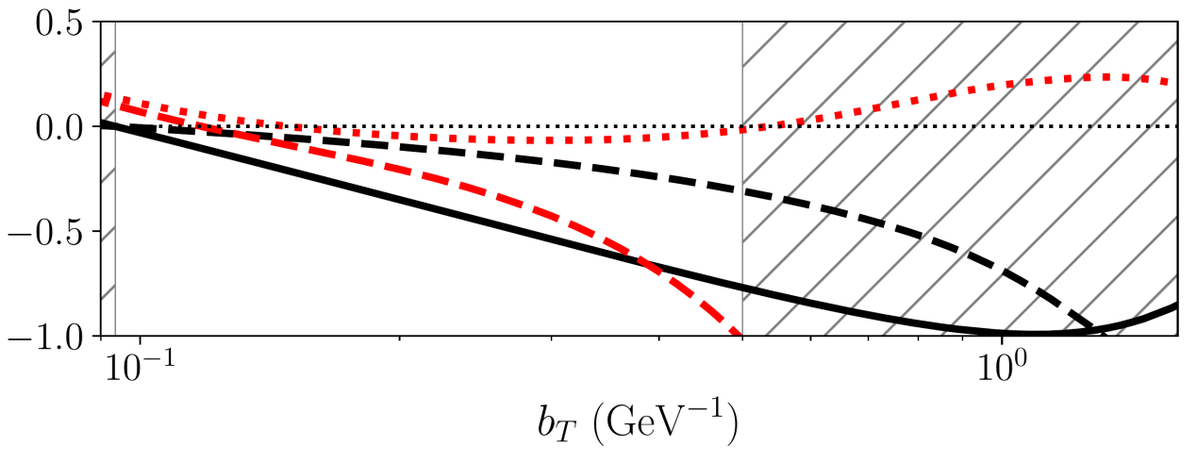
Distorting the perturbative part

Test: $S_P(b_T^*) + S_{NP}(b_T) \simeq S_P(b_T)$ in the perturbative region: $[b_0/Q, b_{T,max}]$ · $b_{T,max}$ = 0.5 GeV^{-1}, S_{NP} from a quark fit × C_A/C_F or × ½

Reminder: $$W^{\rm pert}(b_T) \equiv \tilde{f}_1^g(b_T)\,\tilde{f}_1^g(b_T)\,e^{-S_{\rm P}(b_T)} \to W^{\rm pert}(b_T^*)\,e^{-S_{\rm NP}(b_T)} = \tilde{f}_1^g(b_T^*)\,\tilde{f}_1^g(b_T^*)\,e^{-S_{\rm p}(b_T^*)-S_{\rm NP}(b_T)}$$

Sudakov exponent: NP shift vs perturbative shifts

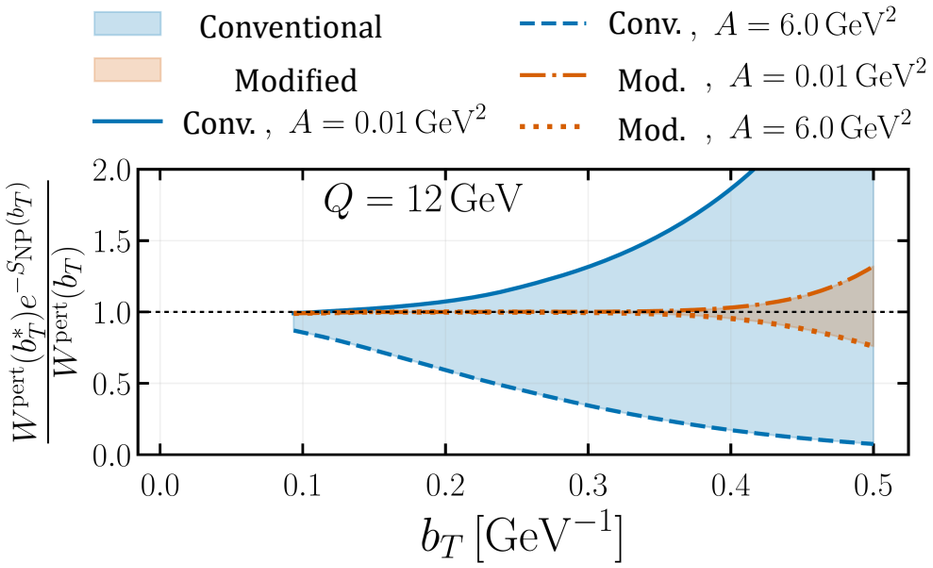
Q = 12 GeV (J/ψ pairs), $b_{T,max}$ = 0.5 GeV^{-1}; white = perturbative region



✗ **Casimir-scaled S_{NP}** (red dashed) deviates far more than LL → NLL → NNLL (black); only the ½-scaled one (dotted) roughly complies → outcome hinges on an S_{NP} not known a priori

Full integrand vs pure perturbative

Q = 12 GeV, scan A ∈ [0.01, 6] GeV²



✗ **Conventional b_T^*** (blue): deviation up to ~100% inside the window

Not a truncation effect: conventional b_T^* + S_{NP} rewrites the perturbative input

Two fit strategies, both with perturbative uncertainty

First time: the perturbative uncertainty enters the fit itself

Scale variations (μ, ζ × 2) and Hessian PDF members act as a theory constraint on the NP parameters A, B

Common setup: NNLL · MSHT20 NLO · $b_{T,max} = 0.5\ \text{GeV}^{-1}$ · $S_{NP} = [A \ln(Q/Q_{NP}) + B]\, b_T^2$, $Q_{NP} = 1\ \text{GeV}$

Two fit strategies, both with perturbative uncertainty

★ First time: the perturbative uncertainty enters the fit itself

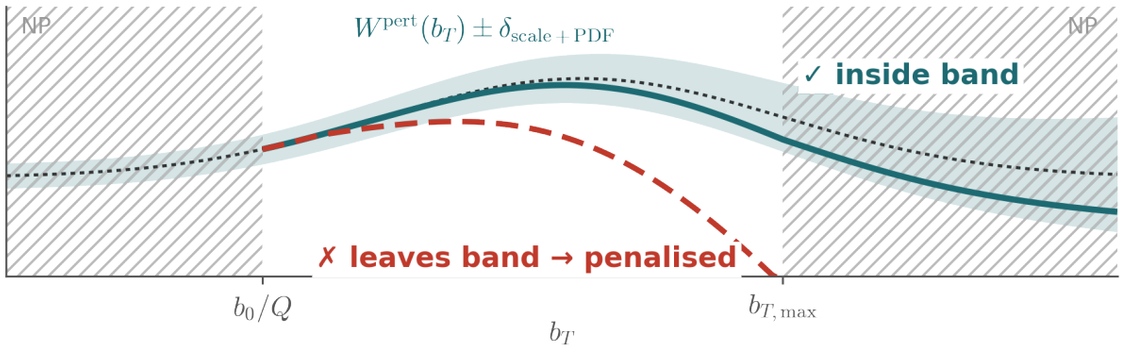
Scale variations (μ, ζ × 2) and Hessian PDF members act as a theory constraint on the NP parameters A, B

Common setup: NNLL · MSHT20 NLO · $b_{T,max} = 0.5\ \text{GeV}^{-1}$ · $S_{NP} = [A \ln(Q/Q_{NP}) + B]\, b_T^2$, $Q_{NP} = 1$ GeV

1 Constraint in b_T space

Conventional b_T^*

The NP model may deform W^{pert} only **within its own perturbative uncertainty band**



$$\chi^2_{b_T} = \chi^2 + D_{\text{pert}}$$

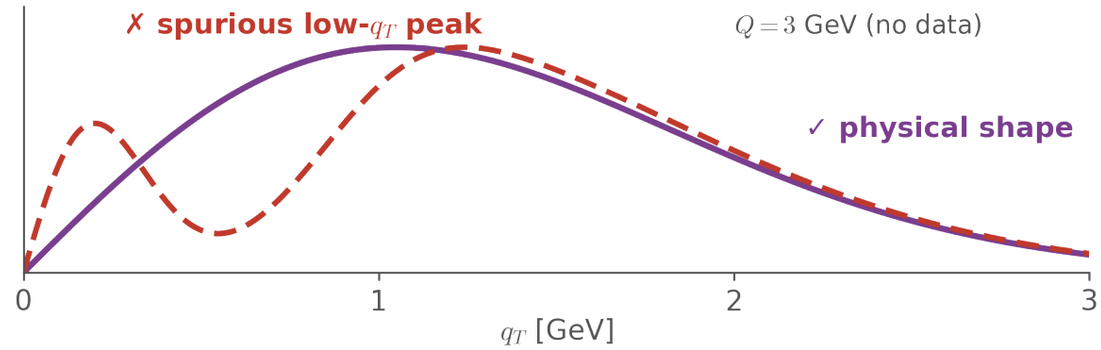
$$D_{\text{pert}} = \sum_Q \left(\tilde{f}_i(\theta) - T_i^0\right) (C_{\text{th}})^{-1}_{ij} \left(\tilde{f}_j(\theta) - T_j^0\right)$$

- **a** **Theory covariance C_{th}**: 9-point scale variation (μ, ζ × 2) + Hessian PDF members, for $b_T \in [b_0/Q, b_{T,max}]$
- **b** **Penalty D_{pert}**: deformation of $W^{pert}(b_T^*)\exp(-S_{NP})$ w.r.t. $W^{pert}(b_T)$, weighted by C_{th}^{-1} (spectrally regularised)
- **c** **Monte Carlo replicas** of data and theory (Gaussian with C_{exp} and C_{th}); minimise χ^2_{bT} for each → mean ± std. dev.

2 Constraint in q_T space

Systematic reduction of the deviation in b_T

NP effects switched off inside the perturbative part; the unphysical oscillations in q_T this induces are forbidden



$$\chi^2_{q_T} = \chi^2 + \lambda \int dq_T \left[\max\left\{0, \left(\frac{1}{\sigma}\frac{d\sigma}{dq_T}\right)''\right\}\right]^2$$

- **a** **Generate 200 theory replicas** (scale + PDF variations)

$$f_k = f_0 + \sum_{s \in \{\mu, \zeta, \text{PDF}_l\}} \frac{f^{(s,+)} - f^{(s,-)}}{2} R_s^k\,, \qquad R_s^k \sim \mathcal{N}(0,1)$$

- **b** **Fit each replica** with χ^2_{qT}: curvature penalty at Q = 3 GeV, $q_T \in [0, 3]$ GeV (no data), $\lambda = 10^7$
- **c** **Reweight with the data** ($N_{eff}/N_{rep} = 0.47$):

$$w_k = \frac{e^{-\chi^2_k/2}}{\frac{1}{N_{\text{rep}}}\sum_i e^{-\chi^2_i/2}}\,, \qquad \langle O \rangle = \frac{1}{N_{\text{rep}}} \sum_k w_k\, O(f_k)$$

Results

Fit results

1 b_T-constrained · n = 2 · NNLL

A [GeV²]	B [GeV²]	χ²/dof
0.36 ± 0.20	1.04 ± 0.68	1.18

≈ compatible

2 q_T-constrained · n = 10 · NNLL

A [GeV²]	B [GeV²]	χ²/dof
0.17 ± 0.06	1.03 ± 0.23	1.03

Fit results

1 b_T-constrained · n = 2 · NNLL

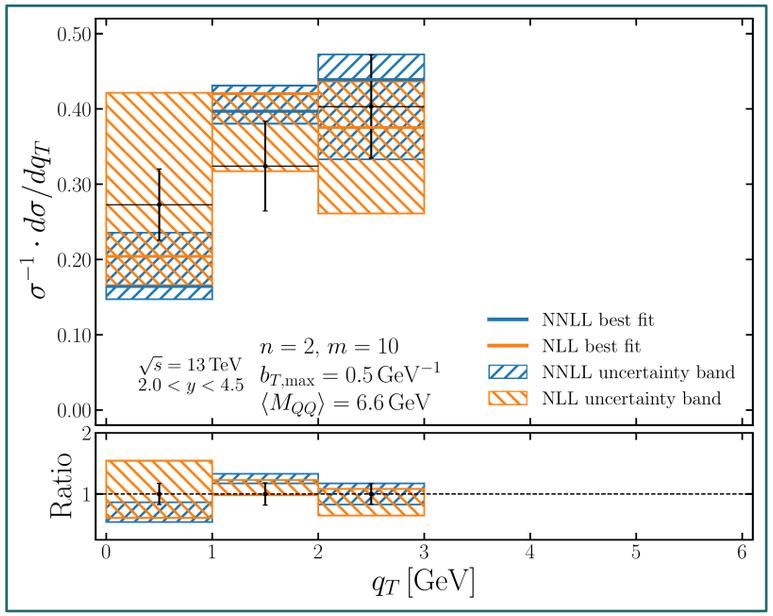
A [GeV²]	B [GeV²]	χ²/dof
0.36 ± 0.20	1.04 ± 0.68	1.18

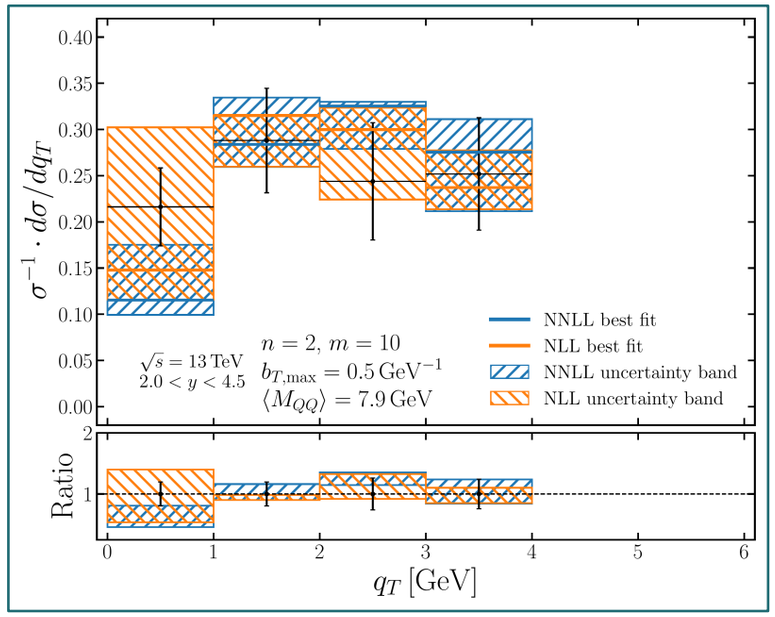
≈ compatible

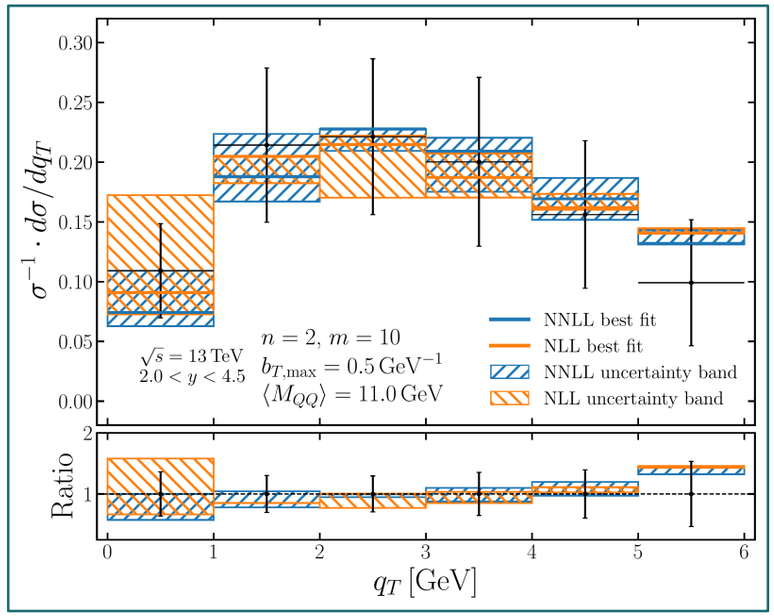
2 q_T-constrained · n = 10 · NNLL

A [GeV²]	B [GeV²]	χ²/dof
0.17 ± 0.06	1.03 ± 0.23	1.03

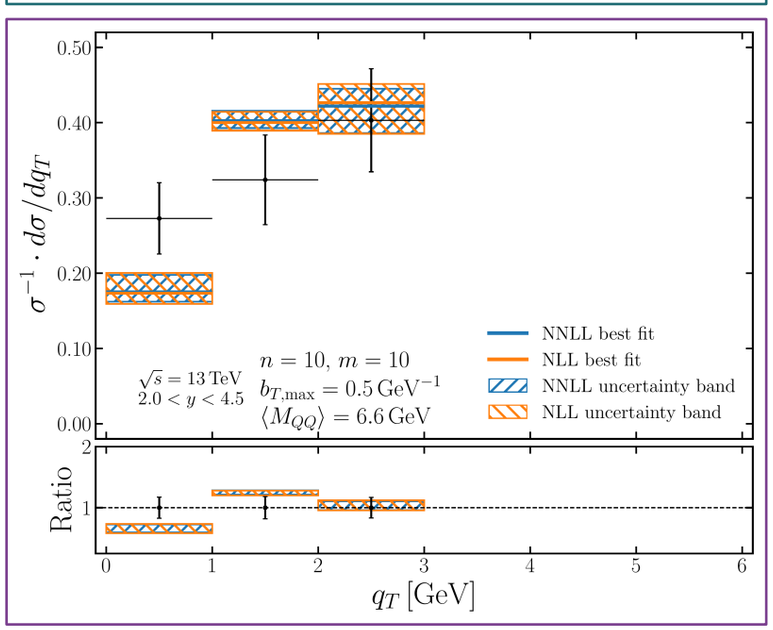
1 b_T-constrained

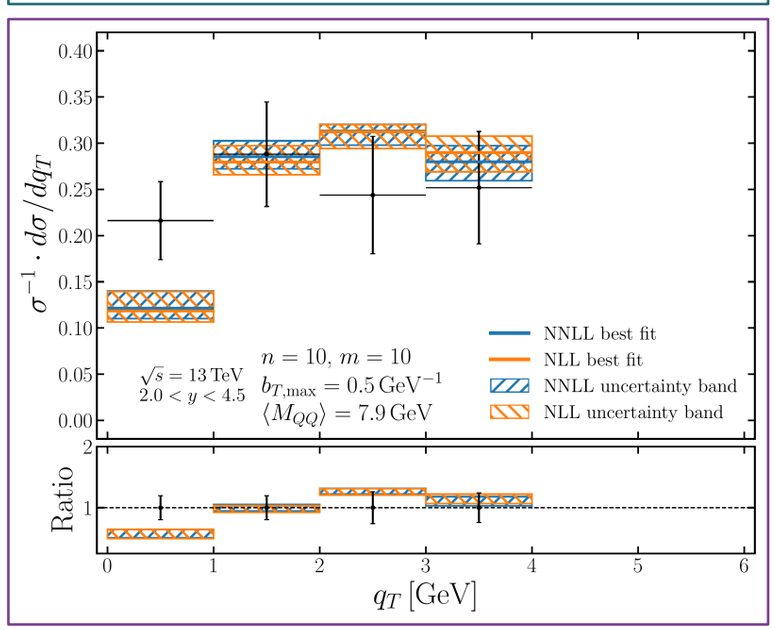


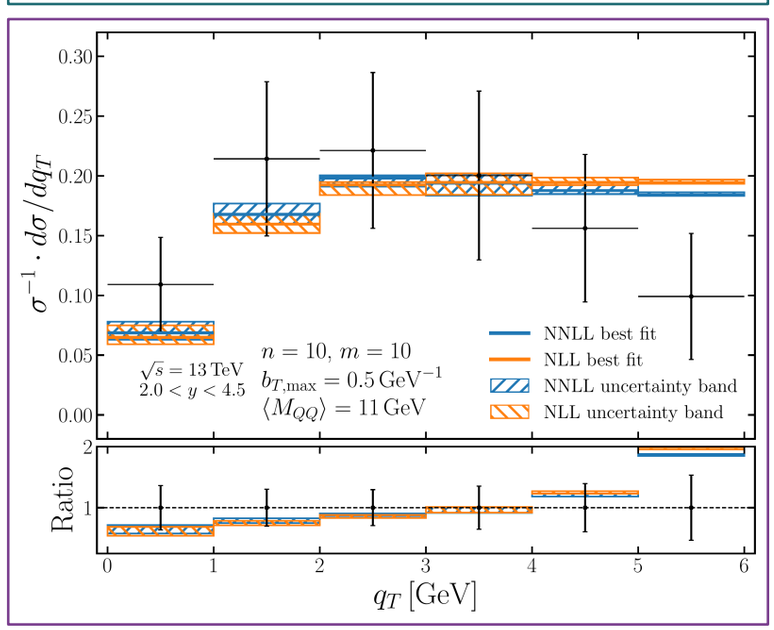




2 q_T-constrained







In each panel: **NNLL** (blue) vs NLL (orange), with LHCb data; compare the rows column by column

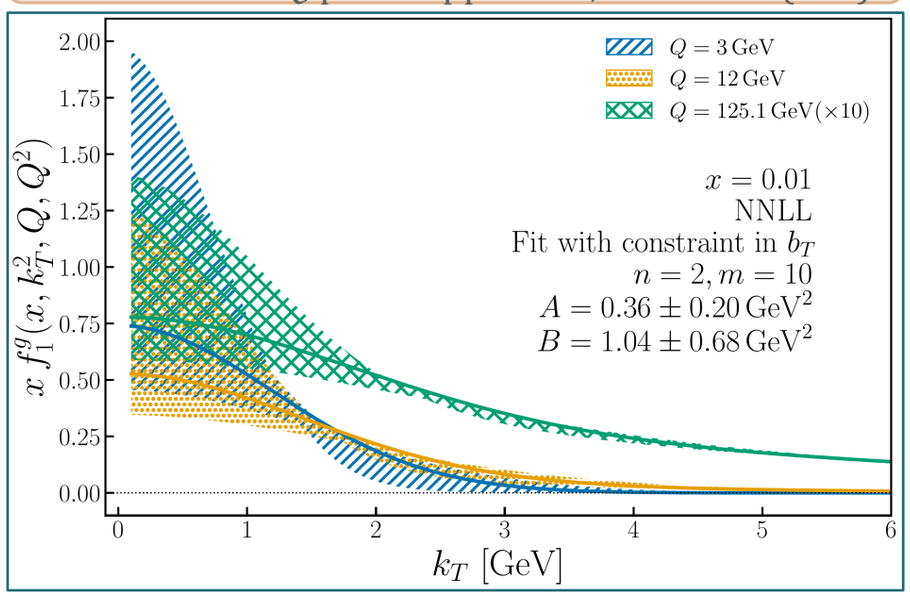
Two independent strategies → a compatible NNLL extraction of A and B

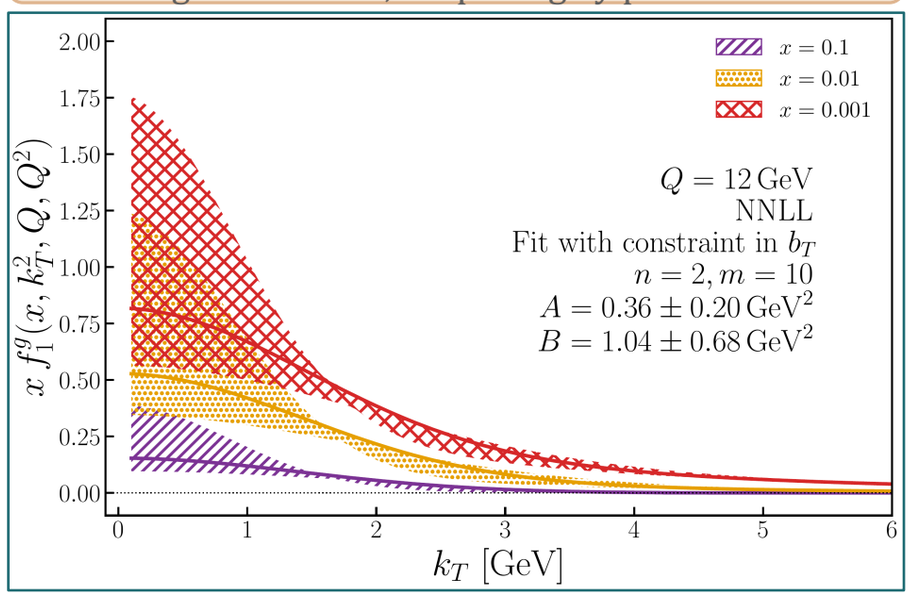
The gluon TMD f_1^g at NNLL

Q dependence (x = 10^{-2})
broadens with Q, peak suppressed; 125.1 GeV (×10)

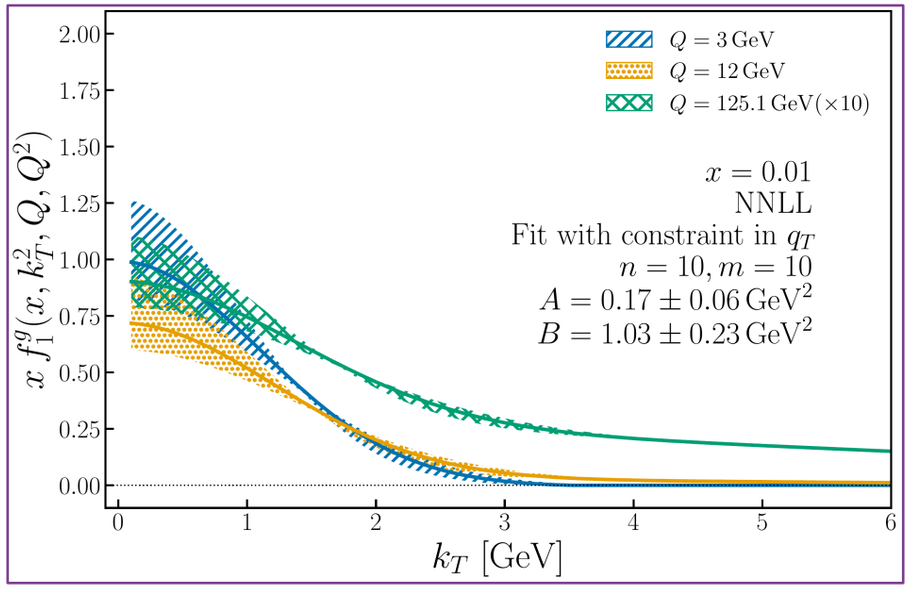
x dependence (Q = 12 GeV)
larger at small x, shape largely preserved

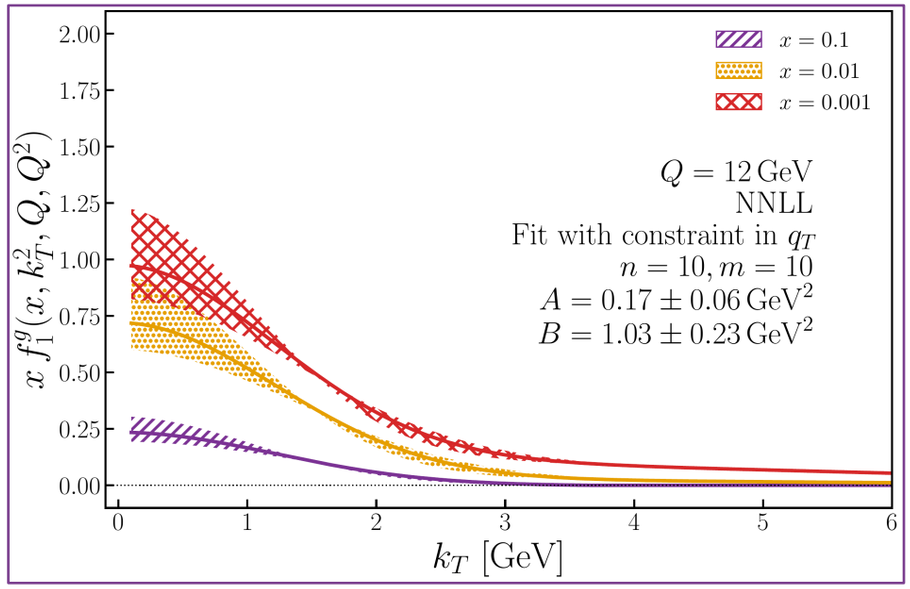
① b_T-constrained





② q_T-constrained





Very similar central curves; ② **gives narrower bands**, mostly at low Q and small k_T
(A, B better constrained)

The gluon TMD f_1^g at NNLL

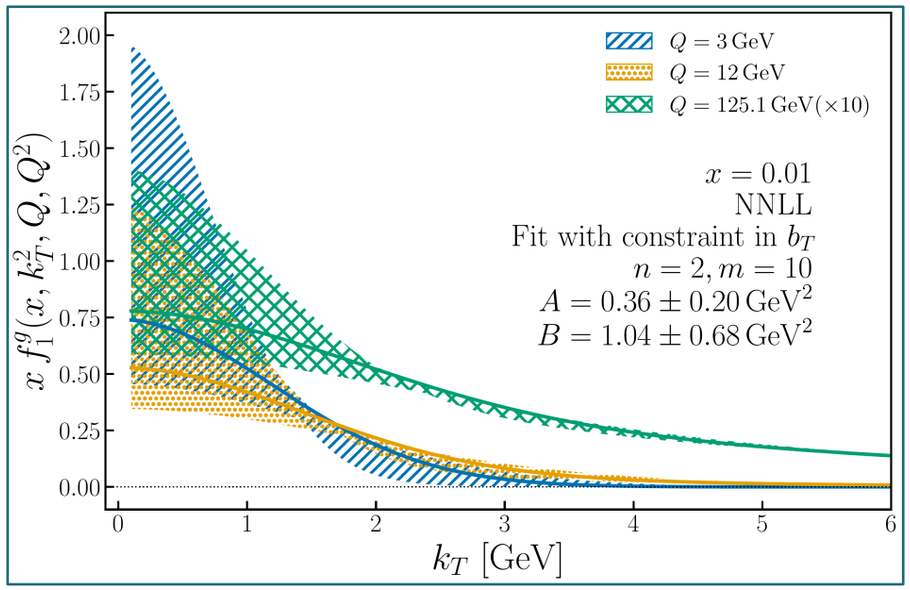
Q dependence (x = 10⁻²)

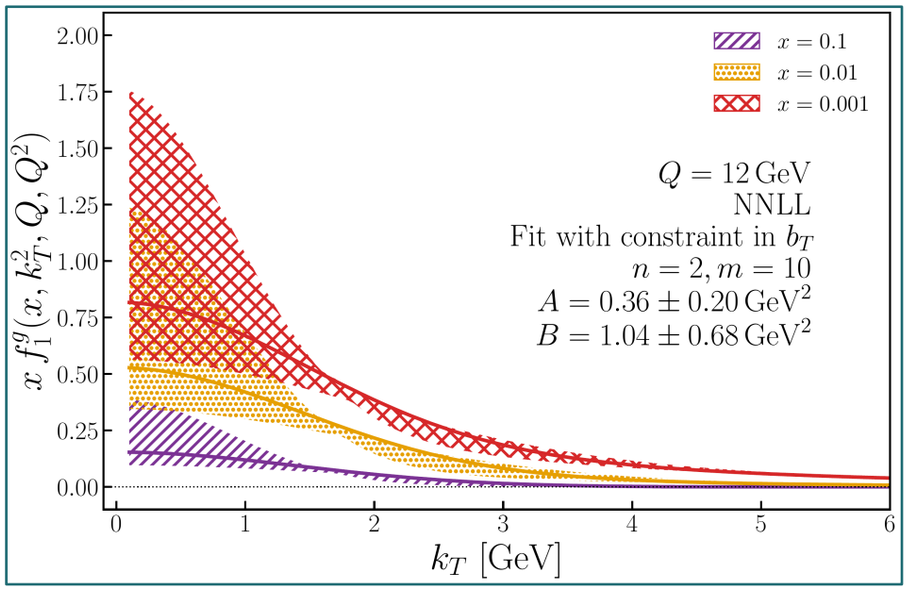
broadens with Q, peak suppressed; 125.1 GeV (×10)

x dependence (Q = 12 GeV)

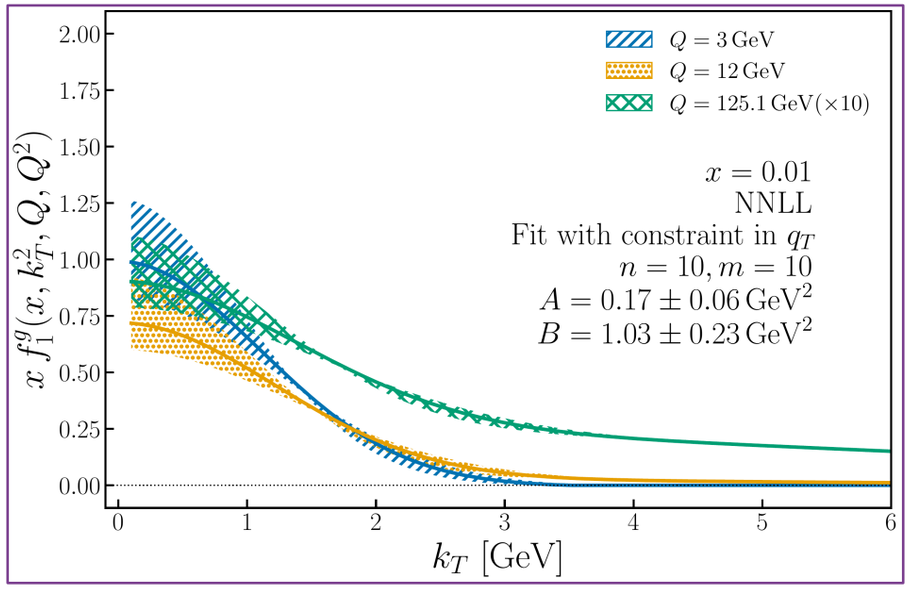
larger at small x, shape largely preserved

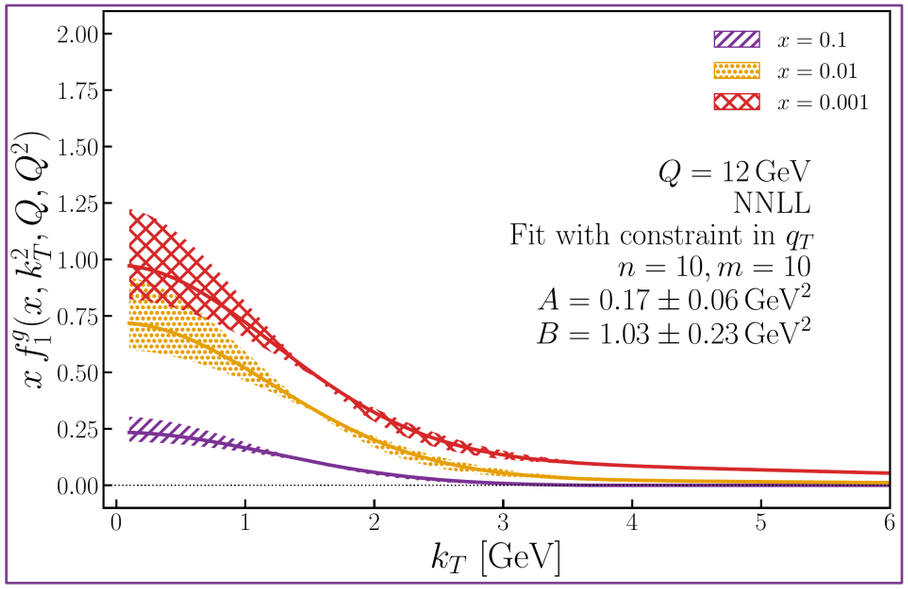
① b_T-constrained





② q_T-constrained





vs Higgs q_T fit

arXiv:2605.28216

✓ **A [GeV²]**

① **0.36 ± 0.20**

Higgs 0.334 ± 0.030

compatible

✗ **B [GeV²]**

① **1.04 ± 0.68**

Higgs 14.4 ± 5.1

incompatible

Different setups

$b_{T,max}$ = 0.5 vs 1.5 GeV⁻¹;
Higgs fit frees B only, A fixed by Casimir scaling from a CS-kernel fit

Larger B

steeper S_{NP} → broader k_T distribution.

Very similar central curves; ② **gives narrower bands**, mostly at low Q and small k_T (A, B better constrained)

The Collins–Soper kernel

NP part fixed by the fitted A

$$\mathcal{D}(b_T,\mu) = \mathcal{D}_{\rm P}(b_T^*,\mu_{b^*}) + \int_{\mu_{b^*}}^{\mu} \frac{\mathrm{d}\mu'}{\mu'}\,\Gamma(\mu') + \mathcal{D}_{\rm NP}(b_T)$$

$$\mathcal{D}_{\rm NP}(b_T) = \frac{A}{4}\, b_T^{\dagger\,2}(b_T)$$

Casimir scaling: exact up to four loops for the perturbative part, extended here to the NP part

$$\mathcal{D}^{(q)}(b_T,\mu) = \frac{C_F}{C_A}\,\mathcal{D}^{(g)}(b_T,\mu) \quad \Rightarrow \quad A^{(q)} = \frac{C_F}{C_A}\,A$$

The Collins–Soper kernel

NP part fixed by the fitted A

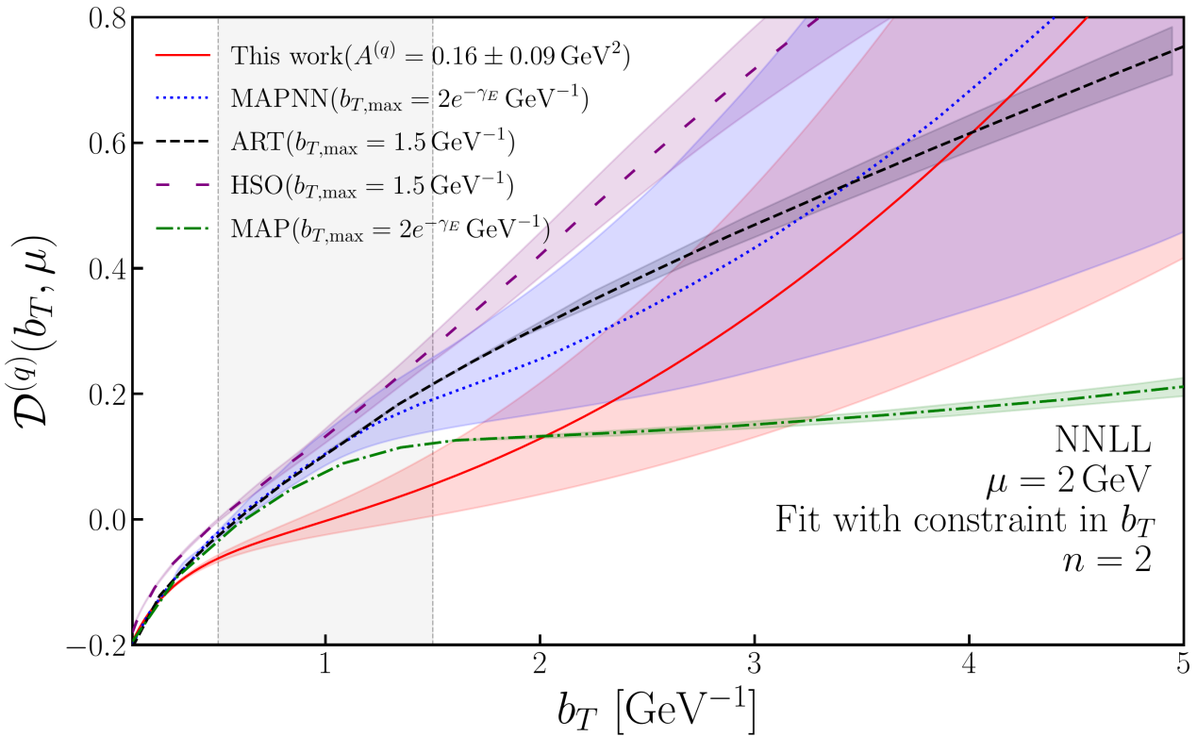
$$\mathcal{D}(b_T,\mu) = \mathcal{D}_{\rm P}(b_T^*,\mu_{b^*}) + \int_{\mu_{b^*}}^{\mu} \frac{\mathrm{d}\mu'}{\mu'}\,\Gamma(\mu') + \mathcal{D}_{\rm NP}(b_T)$$

$$\mathcal{D}_{\rm NP}(b_T) = \frac{A}{4}\, b_T^{\dagger\,2}(b_T)$$

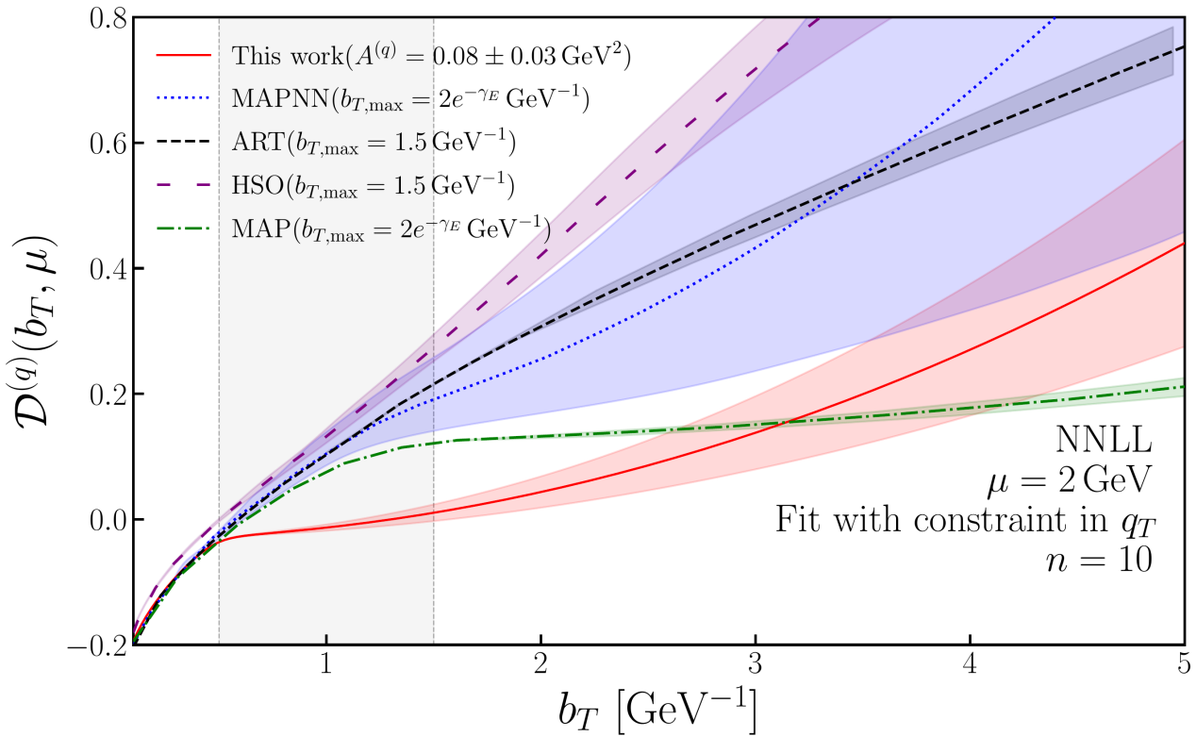
Casimir scaling: exact up to four loops for the perturbative part, extended here to the NP part

$$\mathcal{D}^{(q)}(b_T,\mu) = \frac{C_F}{C_A}\,\mathcal{D}^{(g)}(b_T,\mu) \quad \Rightarrow \quad A^{(q)} = \frac{C_F}{C_A}\,A$$

1 b_T-constrained: $A^{(q)} = 0.16 \pm 0.09$ GeV^2



2 q_T-constrained: $A^{(q)} = 0.08 \pm 0.03$ GeV^2



The Collins–Soper kernel

NP part fixed by the fitted A

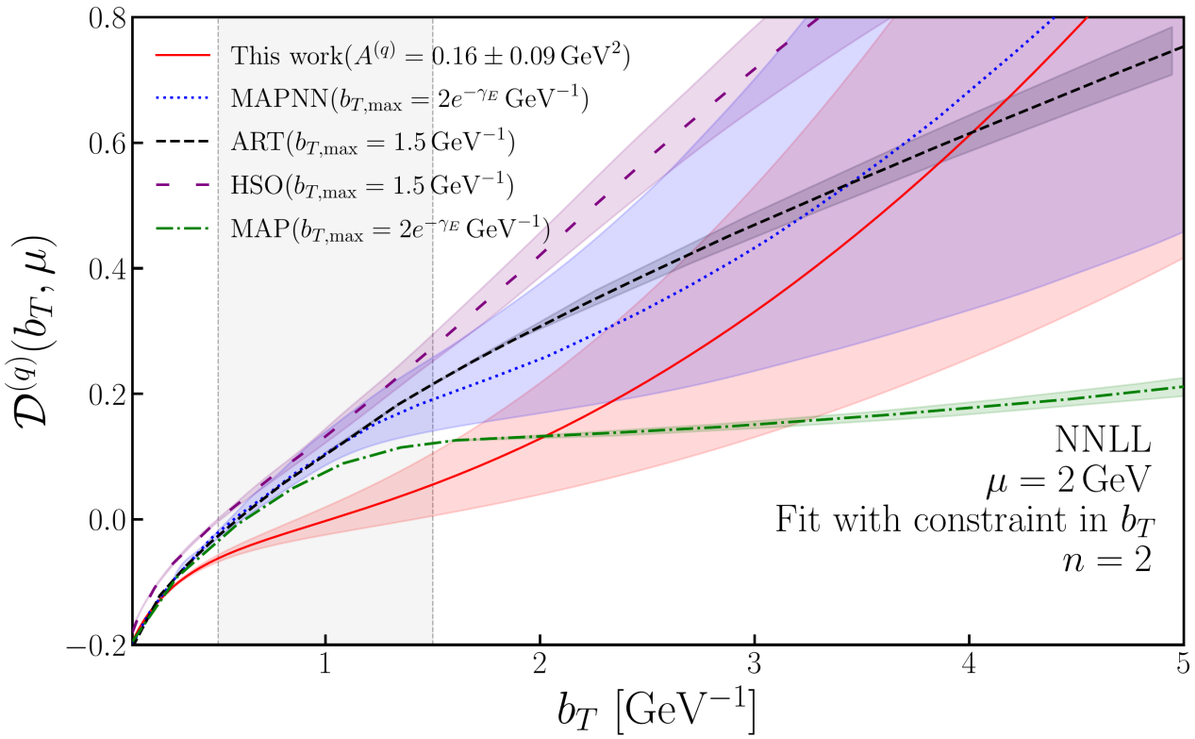
$$\mathcal{D}(b_T,\mu) = \mathcal{D}_{\rm P}(b_T^*,\mu_{b^*}) + \int_{\mu_{b^*}}^{\mu} \frac{\mathrm{d}\mu'}{\mu'}\,\Gamma(\mu') + \mathcal{D}_{\rm NP}(b_T)$$

$$\mathcal{D}_{\rm NP}(b_T) = \frac{A}{4}\, b_T^{\dagger\,2}(b_T)$$

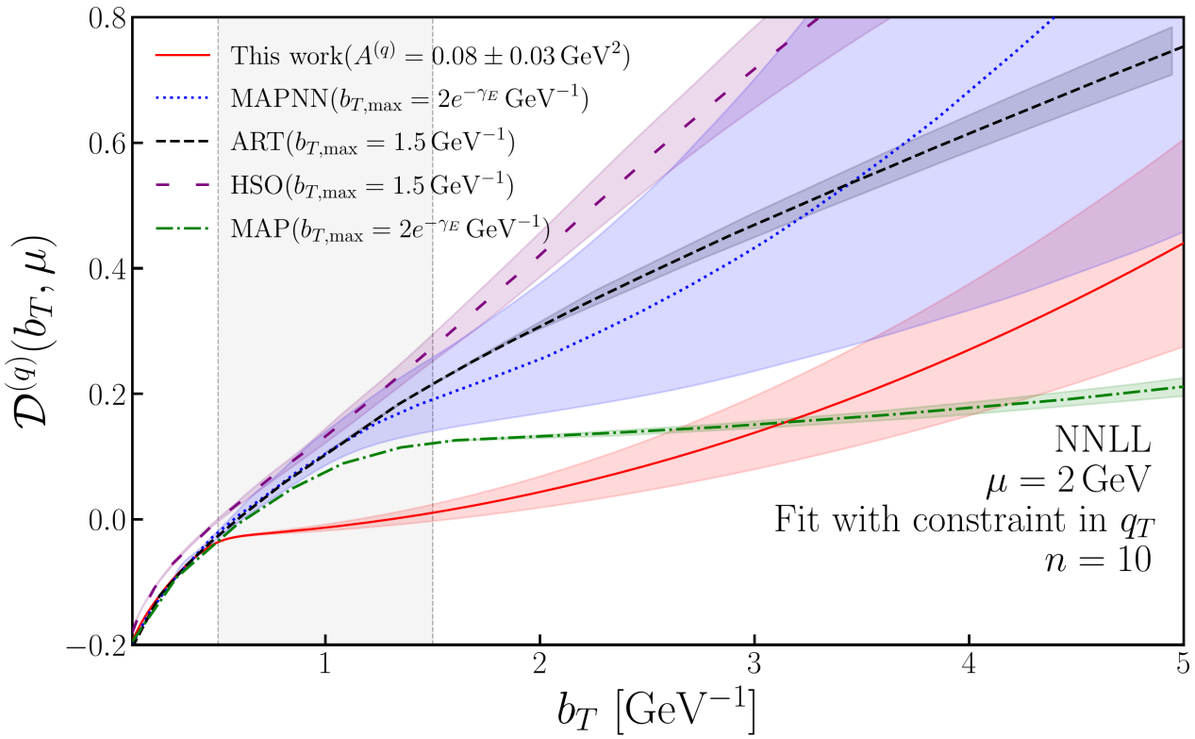
Casimir scaling: exact up to four loops for the perturbative part, extended here to the NP part

$$\mathcal{D}^{(q)}(b_T,\mu) = \frac{C_F}{C_A}\,\mathcal{D}^{(g)}(b_T,\mu) \quad \Rightarrow \quad A^{(q)} = \frac{C_F}{C_A}\,A$$

1 b_T-constrained: $A^{(q)} = 0.16 \pm 0.09$ GeV²



2 q_T-constrained: $A^{(q)} = 0.08 \pm 0.03$ GeV²



✓ **Small b_T**

All determinations agree, as expected in the perturbative region

↗ **Large b_T**

b_T fit: steeper, wider band.

q_T fit: flatter, within the spread of quark extractions

! **Earlier quadratic rise**

Quark fits use smaller A and larger $b_{T,max}$ (grey band): comparison there less direct

Compatible with the more recent fits, in line also with the recent work 2607.24587, while not with the LBNY fit, which used $b_{T,max}$ = 0.5 GeV−1.

LBNY ref.: hep-ph/0212159

The Collins–Soper kernel

NP part fixed by the fitted A

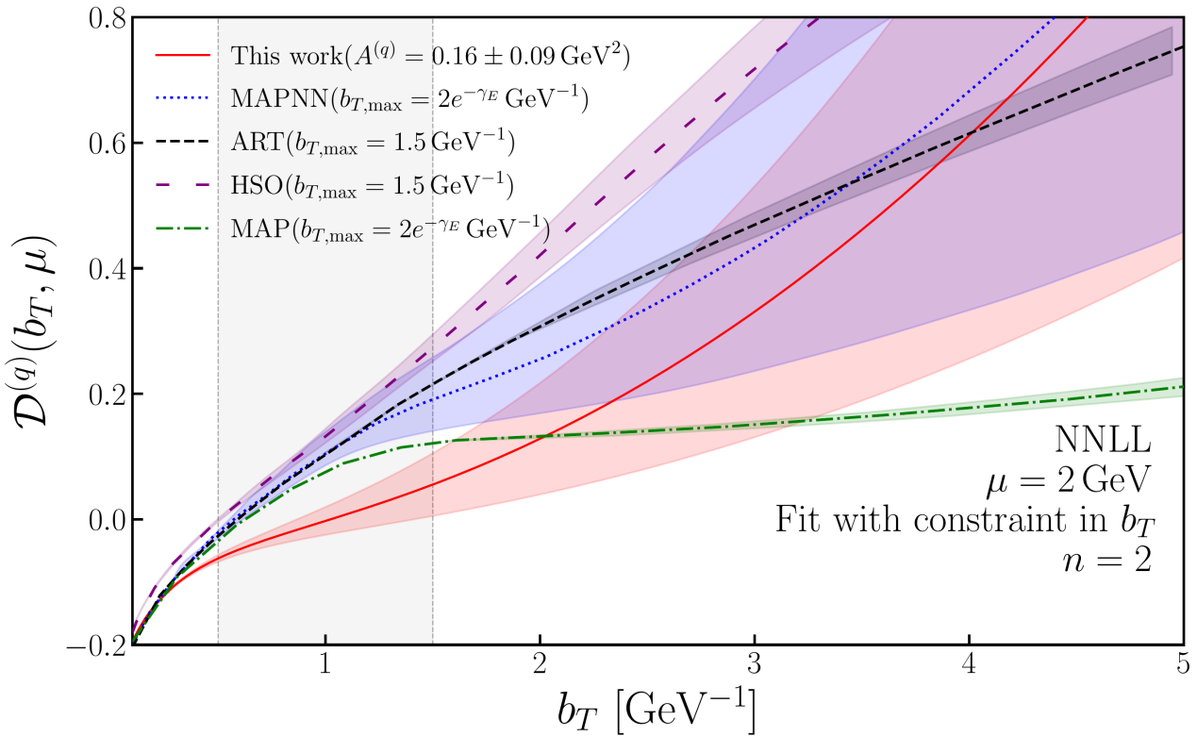
$$\mathcal{D}(b_T,\mu) = \mathcal{D}_{\rm P}(b_T^*,\mu_{b^*}) + \int_{\mu_{b^*}}^{\mu} \frac{\mathrm{d}\mu'}{\mu'}\,\Gamma(\mu') + \mathcal{D}_{\rm NP}(b_T)$$

$$\mathcal{D}_{\rm NP}(b_T) = \frac{A}{4}\, b_T^{\dagger\,2}(b_T)$$

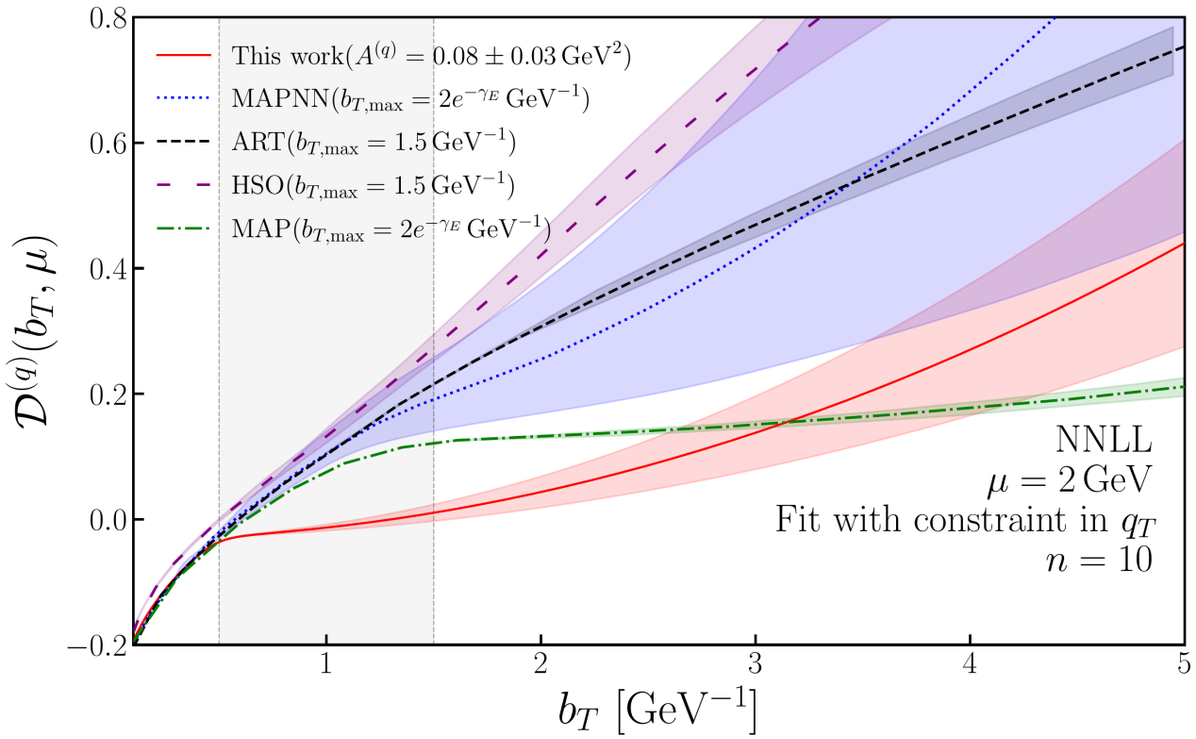
Casimir scaling: exact up to four loops for the perturbative part, extended here to the NP part

$$\mathcal{D}^{(q)}(b_T,\mu) = \frac{C_F}{C_A}\,\mathcal{D}^{(g)}(b_T,\mu) \quad \Rightarrow \quad A^{(q)} = \frac{C_F}{C_A}\,A$$

1 b_T-constrained: $A^{(q)} = 0.16 \pm 0.09$ GeV²



2 q_T-constrained: $A^{(q)} = 0.08 \pm 0.03$ GeV²



✓ **Small b_T**

All determinations agree, as expected in the perturbative region

↗ **Large b_T**

b_T fit: steeper, wider band.

q_T fit: flatter, within the spread of quark extractions

! **Earlier quadratic rise**

Quark fits use smaller A and larger $b_{T,max}$ (grey band): comparison there less direct

Compatible with the more recent fits, in line also with the recent work 2607.24587, while not with the LBNY fit, which used $b_{T,max}$ = 0.5 GeV−1.

LBNY ref.: hep-ph/0212159

NP gluon CS kernel from data: Casimir scaling of the NP part still to be tested

Conclusions

Conclusions and outlook

Conventional NP treatment fails for low-scale gluons

- $b_T^* + S_{NP}$ rewrites the perturbative input beyond its NNLL uncertainty
- Best χ^2/dof (0.30), but an unphysical q_T shape

★ **Theory uncertainty inside the fit, for the first time**

Perturbative + PDF uncertainties; two independent strategies (b_T and q_T space) give **compatible NNLL results**:

1 b_T-constrained	≈	2 q_T-constrained
A = 0.36 ± 0.20 GeV²		A = 0.17 ± 0.06 GeV²
B = 1.04 ± 0.68 GeV²		B = 1.03 ± 0.23 GeV²

First NNLL extraction of f_1^g from J/ψ-pair data

- NP gluon TMD and Collins–Soper kernel from data.
- $h_1^{\perp g}$ contributes < 0.5%
- A agrees with Higgs q_T data, B (k_T width) does not
- Casimir scaling of the NP CS kernel not confirmed
- PDF uncertainties must enter the fit: different sets agree only then
- Agreement with data improves from NLL to NNLL

Low-scale gluon TMD fits need the theory uncertainty inside the fit · arXiv:2609.01000

Conclusions and outlook

Conventional NP treatment fails for low-scale gluons

- b_T^* + S_{NP} rewrites the perturbative input beyond its NNLL uncertainty
- Best χ^2/dof (0.30), but an unphysical q_T shape

★ **Theory uncertainty inside the fit, for the first time**

Perturbative + PDF uncertainties; two independent strategies (b_T and q_T space) give **compatible NNLL results**:

1 b_T-constrained	≈	2 q_T-constrained
A = 0.36 ± 0.20 GeV²		A = 0.17 ± 0.06 GeV²
B = 1.04 ± 0.68 GeV²		B = 1.03 ± 0.23 GeV²

First NNLL extraction of f_1^g from J/ψ-pair data

- NP gluon TMD and Collins–Soper kernel from data.
- $h_1^{\perp g}$ contributes < 0.5%
- A agrees with Higgs q_T data, B (k_T width) does not
- Casimir scaling of the NP CS kernel not confirmed
- PDF uncertainties must enter the fit: different sets agree only then
- Agreement with data improves from NLL to NNLL

Outlook

→ **Refine the constraints**
more scale-variation points; curvature penalty at several √s

→ **Extend the Q reach**
(q_T, Q) double-differential data from other experiments

→ **x dependence of S_{NP}**
LHCb fixed-target (√s ≈ 115 GeV) and y-differential data

→ **Global analysis**
Higgs production and J/ψ-pair production

→ **Linearly polarised gluons**
$\langle \cos 4\varphi_{CS} \rangle$ to access to $h_1^{\perp g}$

Low-scale gluon TMD fits need the theory uncertainty inside the fit · arXiv:2609.01000

Conclusions and outlook

Conventional NP treatment fails for low-scale gluons

- b_T^* + S_{NP} rewrites the perturbative input beyond its NNLL uncertainty
- Best χ^2/dof (0.30), but an unphysical q_T shape

★ **Theory uncertainty inside the fit, for the first time**

Perturbative + PDF uncertainties; two independent strategies (b_T and q_T space) give **compatible NNLL results**:

1 b_T-constrained	≈	2 q_T-constrained
A = 0.36 ± 0.20 GeV²		A = 0.17 ± 0.06 GeV²
B = 1.04 ± 0.68 GeV²		B = 1.03 ± 0.23 GeV²

First NNLL extraction of f_1^g from J/ψ-pair data

- NP gluon TMD and Collins–Soper kernel from data.
- $h_1^{\perp g}$ contributes < 0.5%
- A agrees with Higgs q_T data, B (k_T width) does not
- Casimir scaling of the NP CS kernel not confirmed
- PDF uncertainties must enter the fit: different sets agree only then
- Agreement with data improves from NLL to NNLL

Outlook

→ **Refine the constraints**
more scale-variation points; curvature penalty at several √s

→ **Extend the Q reach**
(q_T, Q) double-differential data from other experiments

→ **x dependence of S_{NP}**
LHCb fixed-target (√s ≈ 115 GeV) and y-differential data

→ **Global analysis**
Higgs production and J/ψ-pair production

→ **Linearly polarised gluons**
$\langle \cos 4\varphi_{CS} \rangle$ to access to $h_1^{\perp g}$

Thank you!

Low-scale gluon TMD fits need the theory uncertainty inside the fit · arXiv:2609.01000

Backup

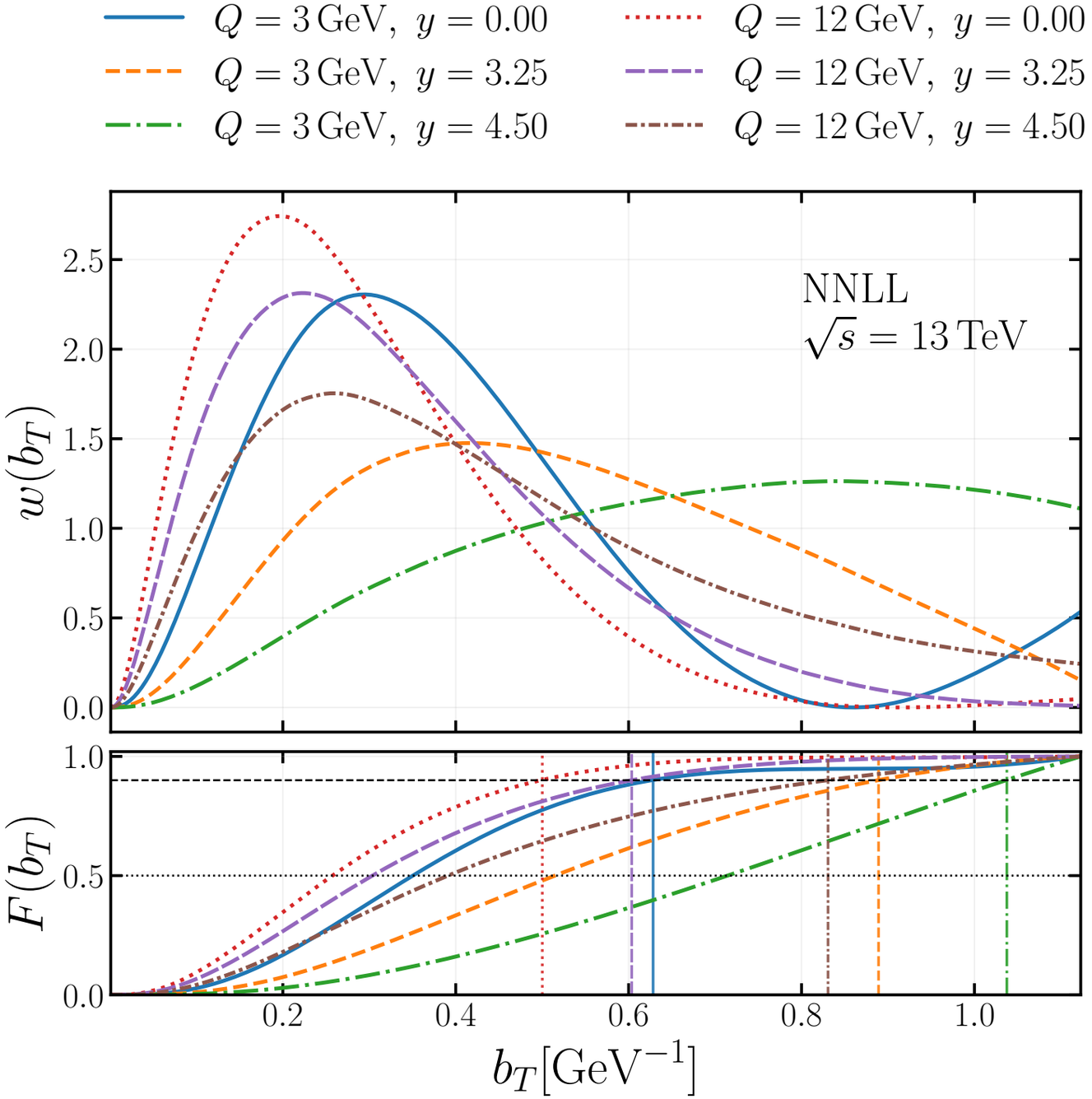
Non-perturbative sensitivity

- $b_{T,max}$ sets the boundary between perturbative and non-perturbative regions; usual choices 0.5–1.5 GeV^{-1}($\mu_b \approx$ 2.25–0.75 GeV)
- Gluons evolve fast (Sudakov $\propto C_A$, two TMDs): narrower perturbative support in b_T than for quarks: $b_{T,max}$ hardly matters
- Large $b_{T,max}$ leaves too much room to perturbative evolution.

$$W_{\text{pert}}(b_T) = \tilde{f}_1^g(x_1, b_T)\tilde{f}_1^g(x_2, b_T)e^{-S_{\text{P}}(b_T)}$$

$$w(b_T) = \frac{b_T W_{\text{pert}}(b_T)}{\int b_T W_{\text{pert}}(b_T)} \qquad F(b_T) = \int_{b_{\text{low}}}^{b_T} w(t)dt$$

- We decide to use $b_{T,max} = 0.5\ GeV^{-1}$



Low $b_{T,max}$: NP sensitivity

Controlling the distortion

- **Goal:** inside [b_0/Q, $b_{T,max}$], perturbative expressions evaluated at $b_T^{'*}$ must coincide with those at b_T

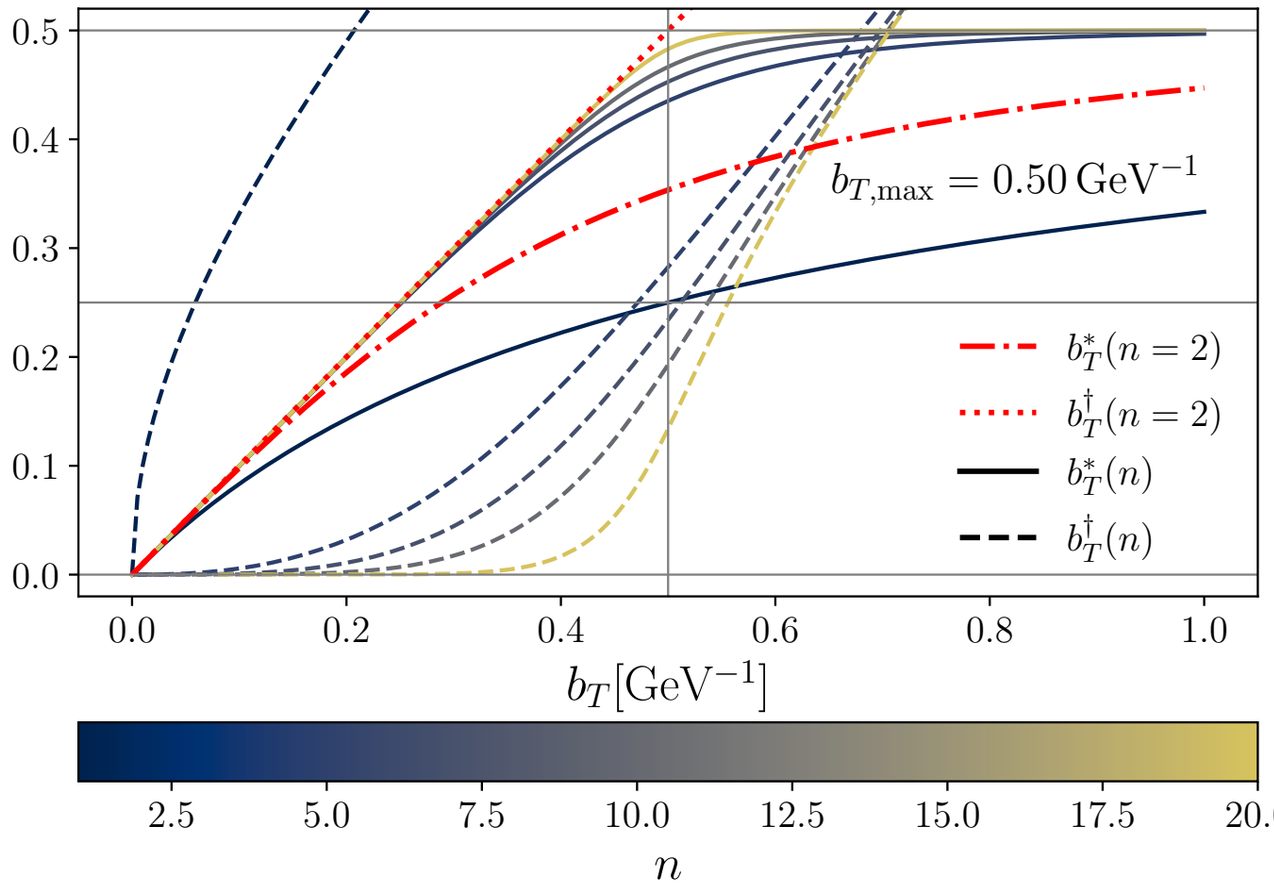
$$b_T^*(n) = \frac{b_T}{\left(1 + (b_T/b_{T,\max})^n\right)^{1/n}} \qquad b_T'(m) = \left(b_T^m + (b_0/Q)^m\right)^{1/m}$$

- n = m = 2 **is the conventional choice.**

- **S_{NP} should act only beyond $b_{T,max}$:** its b_T dependence is replaced by $b_T^\dagger$

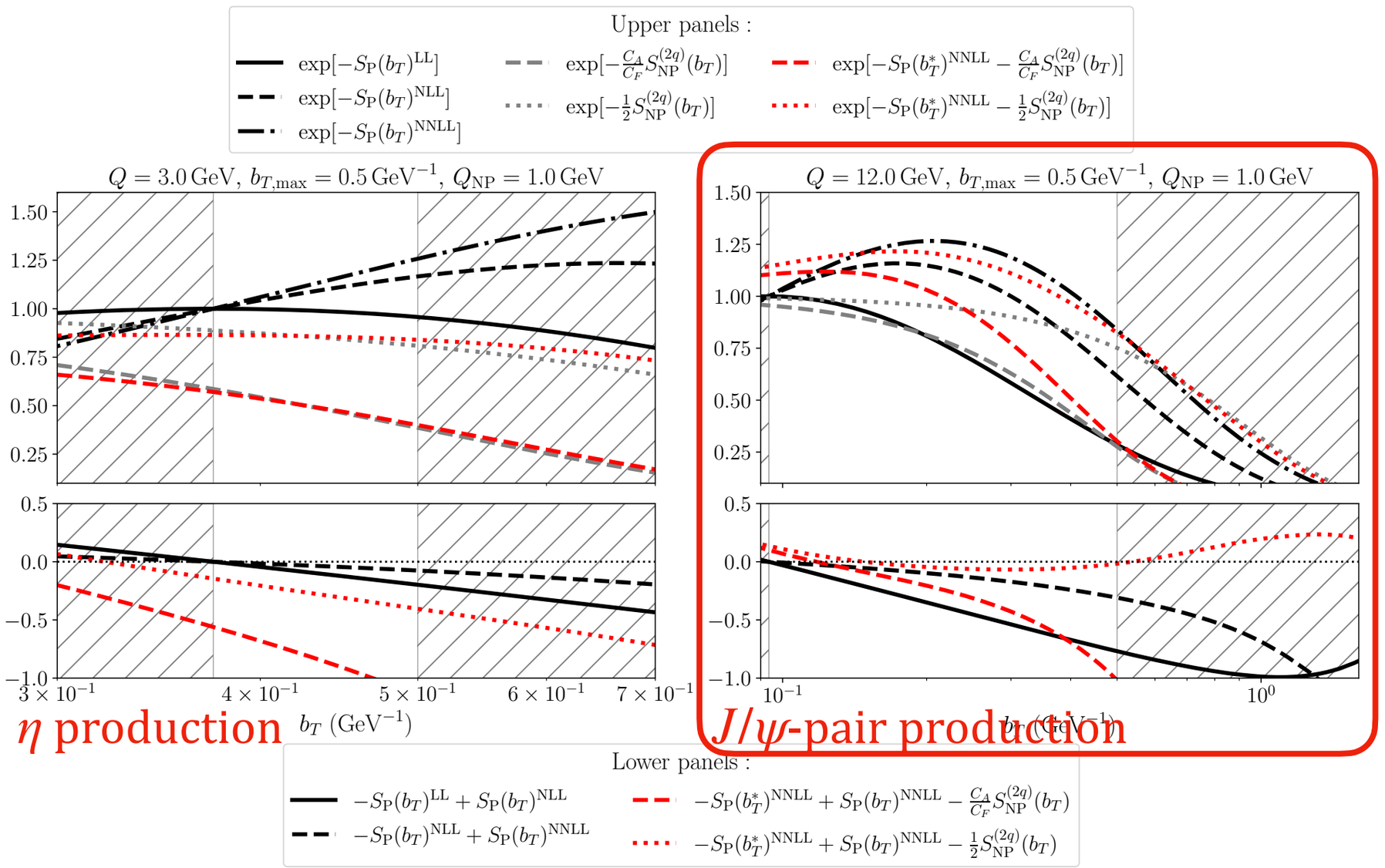
$$b_T^\dagger(n, b_{T,\max}) = \sqrt{\left(b_T^n + b_{T,\max}^n\right)^{2/n} - b_{T,\max}^2}$$

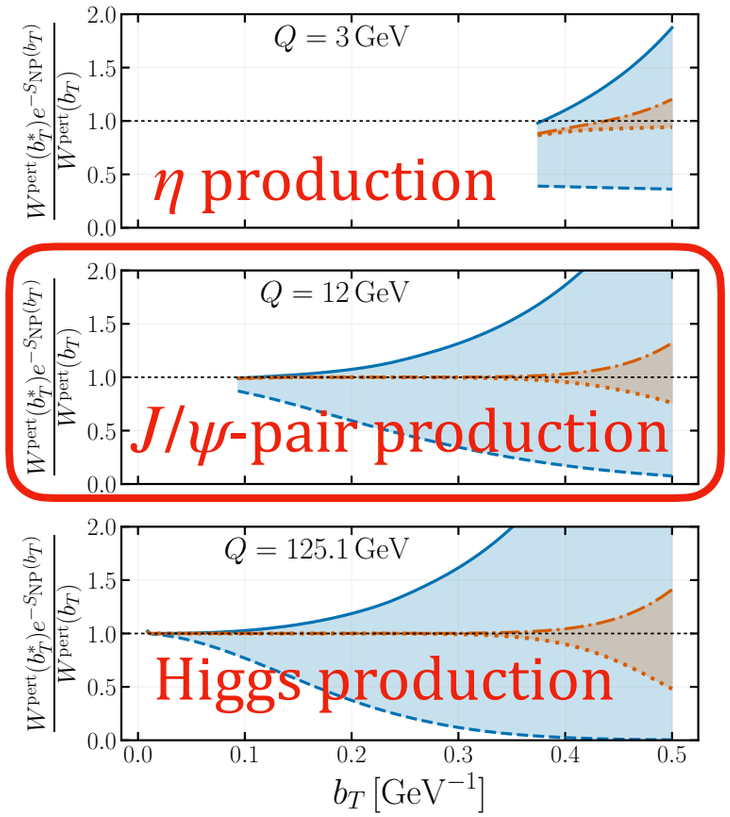
- $b_T^\dagger \to 0$ at small b_T and $b_T^\dagger = b_T$ for n = 2: the **NP factor is switched off inside the window perturbative region.**
- **Systematic reduction** of the deviation of $W^{pert}(b_T^*)\exp(-S_{NP})$ from $W^{pert}(b_T)$.



Perturbative input preserved below $b_{T,max}$; NP effects confined to $b_T > b_{T,max}$

Distorting the perturbative part





$$W^{\rm pert}(b_T) = \tilde{f}_1^g(x_1, b_T)\tilde{f}_1^g(x_2, b_T)e^{-S_{\rm P}(b_T)}$$

- Ideally, **inside the perturbative area** (white): $S_{\rm P}(b_T^*) + S_{\rm NP}(b_T) \simeq S_{\rm P}(b_T)\,, \qquad b_0/Q \le b_T \le b_{T,\max}$
- **Distortion:** $W^{\rm pert}$ is considerably modified in the perturbative area by $b_T^* + S_{\rm NP}$
- The **deviation exceeds the perturbative uncertainty** LL → NLL → NNLL almost everywhere in the perturbative area.

Not a truncation effect: conventional b_T^* + S_{NP} rewrites the perturbative input

Fit results

1 b_T-constrained · n = 2 · NNLL

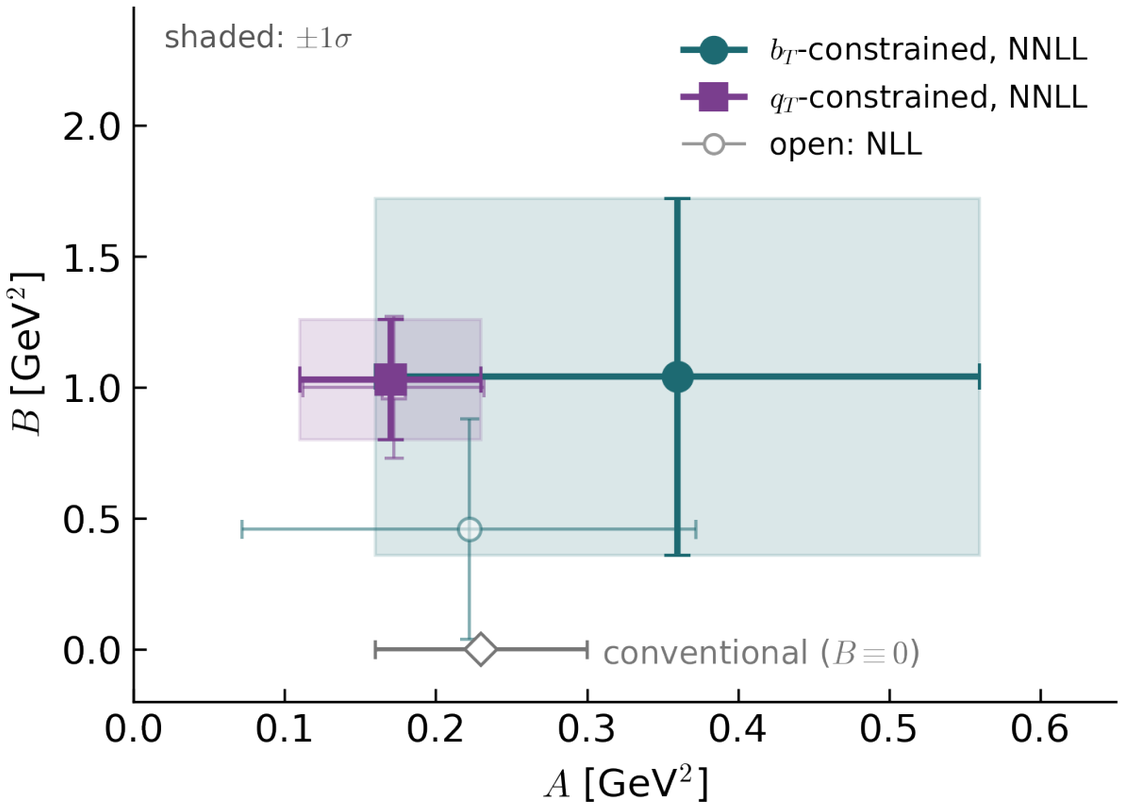
A [GeV²]	B [GeV²]	χ²/dof
0.36 ± 0.20	1.04 ± 0.68	1.18

≈ compatible

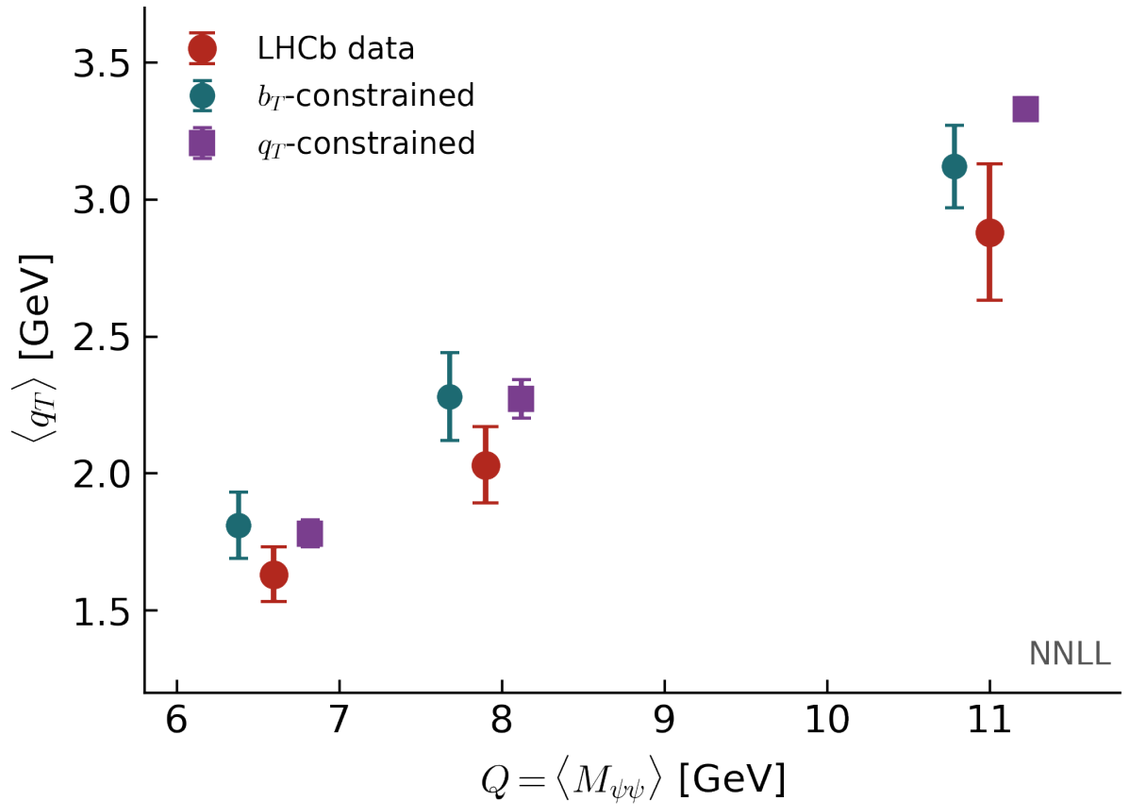
2 q_T-constrained · n = 10 · NNLL

A [GeV²]	B [GeV²]	χ²/dof
0.17 ± 0.06	1.03 ± 0.23	1.03

NNLL parameters overlap within 1σ



…and give the same Q evolution of $\langle q_T \rangle$



NLL → NNLL: stable
A and B unchanged within errors in both strategies (open markers)

NNLL needed for the b_T constraint
At NLL the wider perturbative band weakens D_{pert}: larger errors, χ²/dof = 0.50

Conventional fit
A = 0.23 ± 0.07, χ²/dof = 0.30, but B unconstrained and an unphysical q_T shape

Two independent strategies → a compatible NNLL extraction of A and B